APPLICATIONS FOR ADVANCED OXIDATION OF DRINKING WATER USING UV LEDs

by

Jin Li

Submitted in partial fulfillment of the requirements
for the degree of Master of Applied Science

at

Dalhousie University
Halifax, Nova Scotia
March 2024

Table of Contents

LIST OF TABLES

LIST OF FIGURES

ABSTRACT

Advanced oxidation processes (AOPs) have received much attention in recent years as a new technology for drinking water treatment due to their ability to efficiently degrade natural organic matter (NOM). Ultraviolet light-emitting diode (UV-LED) technology is the most ideal light source for AOPs because of their small size and versatility in design. The focus of this research was to investigate the feasibility of UV-LEDs AOPs in drinking water treatment applications by using pilot-scale treated water from the J. Douglas Kline Water Supply Plant (JDKWSP) which draws water from Pockwock Lake. The research directions were mainly categorized as follows:

(1) To explore the effects of novel UV-LED AOPs as well as conventional ozone reactions on the transformation of NOM in drinking water.
(2) Investigation of changes in the composition of water after AOPs and its association with DBPFP.
(3) To compare three AOP technologies including ozone, UV-LEDs/H_2O_2 and UV-LEDs/Cl_2, for the treatment of water from three different locations in the drinking water treatment process.

In each experiment, 280nm UV-LEDs were used as the experimental light source to complete the experiments at bench-scale, and the UV fluence was adjusted to 100, 500, and 1,000mJ/cm^2 respectively. The overall goal was to help determine the feasibility of UV-LEDs AOPs in water treatment.

The results of the research demonstrated that UV-LEDs AOPs at a fluence of 1000mJ/cm^2 and 10mg/L H_2O_2 or Cl_2 performed better than 10mg/L ozone alone with regards to reducing the SUVA, indicating the partial oxidation of NOM. In particular, the UV-LEDs/Cl_2 reaction achieved the best results for NOM degradation. However, in the case of trihalomethane formation potential (THMFP), ozonation at a dose of 10 mg/L outperformed UV-LEDs AOPs (1000mJ/cm^2 UV with 10mg/L H_2O_2 or Cl_2), however this conclusion needs to be confirmed by additional bench and pilot-scale studies. In summary, UV-LEDs AOPs show great potential and value for future applications in drinking water however their impact on DBPFP should be further characterized.

LIST OF ABBREVIATIONS AND SYMBOLS USED

AC – Activated carbon

Alum – Aluminum sulfate

Ant-Sand – Anthracite-Sand

AOPs – Advanced Oxidation Processes

Cl_2 – Chlorine

cm – Centimeter

DBPFP – Disinfection by-product formation potential

DBPs – Disinfection by-products

DOC – Dissolved organic carbon

DOM – Dissolved organic matter

EEM – Excitation-emission matrix

Em – Emission spectra

Ex – Excitation spectra

FEEM – Fluorescence excitation-emission matrices

FP – Formation potential

FRI – Fluorescence regional integration

g/L – Gram per liter

GAC – Granular activated carbon

GAC-Ant-Sand – GAC-Anthracite-Sand

GC – Gas Chromatograph

H_2SO_4 – Sulfuric acid

HAA – Haloacetic acid

HAAFP – Haloacetic acid formation potential

HPLC – High-performance liquid chromatography

JDKWSP – J. Douglas Kline Water Supply Plant

LP – Low pressure

mg/L Milligram per liter

mL/min – Milliliter perminute

mm – Millimeter

MP – Medium pressure

MW – Molar Weight

nA – Nanoampere

Na_2SO_4 – Sodium sulfate

NaOH – Sodium hydroxide

NOM – Natural organic matter

PAC – Powdered activated carbon

pCBA – Para-chlorobenzoic acid

SUVA – Specific ultraviolet absorbance

THM – Trihalomethane

TOC – Total organic carbon

UFC – Uniform Formation Potential

UV254 – The ultraviolet absorbance of water at a UV wavelength of 254 nanometers (nm)

UV-LEDs – Ultraviolet light emitting diodes

UV-Vis – UV-visible

UV-Vis Abs – UV-visible absorbance

V – Volt

μA – Microamp

μg/L – Microgram per liter

μm – Micrometer

μs – Microsecond

ACKNOWLEDGEMENT

First and foremost, I am very happy to have had the opportunity to study and complete a graduate program at Dalhousie University in Canada, which would not have been possible without my supervisor, Dr. Graham Gagnon. He not only helped me a lot in the research process, but also helped me to better understand the meaning of research and my own potential.

However, my journey to graduate school would not have been as easy without the help of Dr. Lindsay Anderson. She not only welcomed and encouraged me when I came to the lab, gave me a lot of advice on the details of my experiments, and gave me a lot of help and joy in my life. She made me feel that working at CWRS is a joy and not just a task.

And luckily, I was also mentored by Dr. Sean MacIsaac and Jessica Bennett. They gave me invaluable advice and help in the planning and execution of my experiment. In addition to their guidance, all of the experiments would not have been possible without Heather Daurie. I would also like to thank Heather for putting up with all the troubles I caused lol. I would also like to thank the staff and co-op students who worked hard behind the scenes, such as Valentin, Jeffery, Manda, Jodi, Chantelle, and others.

I am happy to work at CWRS not only because I have a group of kind coworkers, but also because they are my beloved friends. I would like to thank Aaron, Ryan, Naomi, Emma, and others for helping me along the way and for the fun times I had. My short time as a graduate student will be over, but I hope the memories of our fun times will last forever.

Finally, I would like to thank my parents across the ocean for the support and encouragement they have given me for so long. The road ahead is long and difficult, but with you by my side, all the difficulties should be solved without a hitch.

Chapter 1: Introduction

1.1 Background

Global climate change is affecting our environment and drinking water production is no exception. (Program, 2009). One of the more significantly impacted aspects is on drinking water supplies, and particularly the concentration of natural organic matter (NOM). For Atlantic Canada, the impacts of climate change on water resources mainly affect surface water supplies (Delpla et al., 2009; Whitehead et al., 2009). According to recent studies, NOM in drinking surface water sources in this region has shown an increasing trend, especially in the Nova Scotia region (Anderson, DeMont, et al., 2023; Anderson et al., 2017).

Elevated NOM has a direct impact on the amount of aluminum based coagulant in the treatment process, which increases the cost of operating the treatment plant and creates the risk of high residual aluminum levels (Matilainen et al., 2010; Anderson et al., 2017). In addition to the increased amount of coagulant, the increased amount of organic matter can also cause problems such as algal toxins, higher levels of bacteria, and various water quality issues (Anderson, DeMont, et al., 2023). The direct effect of increased NOM, its effect on DBPs, which are harmful substances produced by the reaction of chlorine with NOM in water due to the unavoidable chlorine disinfection part of the water treatment process, is also apparent (Boorman, 1999; Singer, 1994; Srivastav et al., 2020). Therefore, the necessary measures for decreasing NOM in water must be implemented to adapt to

future climate change (Anderson, DeMont, et al., 2023).

Advanced oxidation technology is a drinking water treatment technology that has recently received attention with its thorough reaction, high applicability, and potential for degrading difficult-to-treat macromolecules of organic matter into small molecules (Andreozzi et al., 1999; Suty et al., 2004). The traditional advanced oxidation technologies used in water treatment are generally Fenton-related, ozone-related, and hydrogen peroxide-related (Gil et al., 2019; Parsons, 2004). Fenton-related technologies are generally unsuitable for drinking water treatment due to the introduction of hard-to-treat compounds that negatively impact the water column (Jarvis et al., 2008). Since chlorine is already present in the water treatment process, this paper also discusses chlorine-related advanced oxidation technologies as another potential option.

In order not to introduce more compounds in the advanced oxidation of hydrogen peroxide with chlorine, this study used UV light as an excitation energy source to complete the advanced oxidation (Farzanehsa et al., n.d.; Miralles-Cuevas et al., 2017; Rosenfeldt et al., 2006). Unlike the traditional use of mercury lamps to accomplish advanced oxidation, this thesis will investigate UV-LEDs as the UV light source (S. MacIsaac, 2021). Compared to mercury lamps, UV-LEDs produce a more concentrated wavelength, is more compact, and can be more easily installed and used with equipment (Song et al., 2016). However, due to its difference from mercury lamps, the mechanism of UV-LEDs advanced oxidation still needs some exploration.

Therefore, this thesis will explore the mechanism of UV-LEDs related AOPs, comparing the three different oxidation technologies. Including UV-LEDs/H_2O_2, UV-LEDs/Cl_2 and ozone, It will also consider the location of advanced oxidation in the drinking water treatment process, the impact on the water body and the impact of DBPs, and then comprehensively evaluate the application of advanced oxidation for drinking water treatment.

1.2 Research Rationale

The value of this study is to analyze the strengths and weaknesses of advanced oxidation technologies by comparing different advanced oxidation technologies applied to the treatment of drinking water and to measure the feasibility of their installation sites in the water treatment process. The ultimate direction of the research is to help determine whether UV-LEDs AOPs can help water treatment systems build resilience and reduce NOM as well as DBPs in a future of increasing water treatment challenges.

1.3 Research Objectives

The main objectives of the work presented in this thesis document are as follows:

- Explore the effects of novel UV-LEDs AOPs as well as conventional ozone reactions on NOM in drinking water.
- Investigation of changes in the composition of water after AOPs and its association with DBPFP
- Comparing of three advanced oxidation technologies, ozone, UV-LEDs/H_2O_2 and UV-LEDs/Cl_2, for the treatment of water from three different locations in the drinking water treatment process.

1.4 Organization of Thesis

Chapter 2 summarizes a summary of literature studies on the effects of global warming on drinking water, limitations of existing technologies, advanced oxidation technologies, and UV-LED technologies. The goal of this chapter is to give the reader context about the significance of the study as well as the context.

Chapter 3 describes all the experimental methods and experimental designs used in this thesis, including all the instruments, and all the parameters measured.

Chapter 4 investigates novel UV-LEDs AOPs as well as conventional ozone reactions on NOM in drinking water, and after analyzing their principles, compared the three AOPs in many ways using various parameters and talk about their prospects.

Chapter 5 completes the summary of all the experimental results of this paper and points out the shortcomings of the current experiments as well as possible directions for future experiments.

Chapter 2: Literature Review

2.1 Natural Organic Matter

Natural organic matter (NOM) is generally a mixture of organic compounds typically found in groundwater and surface water (Dobrović et al., 2007). NOM is primarily produced by, but not limited to, leaf litter in the water and normal organic biological metabolism (X. Yang et al., 2013). Due to the complexity of its source, NOM in water also generally has a heterogeneous composition (Selberg et al., 2011) Moreover, its content is more related to the climate, especially the temperature, as the metabolism of organic life forms changes with the temperature (Prasad et al., 2020a).

2.1.1 Parameters

The concentration of organic matter in water is usually determined by the Total Organic Carbon (TOC), while Dissolved Organic Carbon (DOC) determines the amount of dissolved organic matter in water as classified by filtration through a 0.45-micron filter paper (Steinberg, 2003). TOC and DOC can indicate the content of organic matter in water. However, it is not possible to analyze the composition and type of organic matter with certainty, so there is a need to combine the use of excitation-emission matrix fluorescence spectroscopy (FEEM), ultraviolet and visible absorption spectroscopy (UV-Vis), and other measurement methods to determine the characteristics of NOM in water in more detail (Dobrović et al., 2007; Steinberg, 2003).

Ultraviolet and visible (UV-Vis) absorption spectroscopy plays a vital role in analyzing organic matter in water (Matilainen et al., 2011). The concentration of a specific substance (analyte) dissolved in a solution can be determined by measuring the attenuation rate of light as it passes through a sample or is reflected from its surface. The versatile technique allows absorbance measurements to be made at a single wavelength or over a wide spectral range. Typically, wavelengths between 220 and 280 nm are best suited for NOM measurements (Hur et al., 2006). However, due to the wide variety of NOM species and their relatively complex structures, the luminescent chromophores they contain vary with different species of NOM. Different wavelengths recognize these different chromophores (Prasad et al., 2020a). The absorbance at 220 nm is related to carboxyl and aromatic chromophores, while the absorbance at 254 nm is related to aromatic groups with different degrees of activation. It is worth noting that although UV_{254} primarily represents aromatic features, it has become an alternative measurement for DOC analysis in the general literature (Matilainen & Sillanpää, 2010; X. Yang et al., 2013).

2.1.2 Composition

NOM can be categorized into two main properties: hydrophobic and hydrophilic (Edzwald, 1993). On average, about 45% of DOC in rivers and lakes is composed of hydrophobic aquatic humus, but the exact proportion is uncertain and is also governed by various factors (Thurman, 2012). The fractionation method for determining the proportion of organic matter in water is referred to as the Leenheer method described by Marhaba (Leenheer et al., 1982; Leenheer & Noyes, 1984; Steinberg, 2003). The standard classifications and chemical compositions of NOM in lakes and rivers are listed in Table 2-1 for reference.

Table 2-1 Natural Organic Matter Fractions (Edzwald, 1993)

Fraction	Chemical Groups
Hydrophobic	
Acids	Humic and fulvic acids, high MW alkyl monocarboxylic and dicarboxylic acids, aromatic acids, phenols, tannins, intermediate MW alkyl monocarboxylic and dicarboxylic acids
Bases	Proteins, aromatic amines, high MW alkyl amines
Neutrals	Hydrocarbons, aldehydes, high MW methyl ketones and alkyl alcohols, ethers, furans, pyrrole
Hydrophilic	
Acids	Hydroxy acids, sugars, sulfonic, low MW alkyl monocarboxylic and dicarboxylic acids
Bases	Amino acids, purines, pyrimidines, low MW alkyl amines
Neutrals	Polysaccharides: low MW alkyl alcohols, aldehydes, and ketones

Recently, fluorescence spectroscopy has increasingly detected organic matter in water (Trueman et al., 2016). Fluorescence spectrometry is typically used to analyze samples through FEEM instruments (Korshin et al., 1999). Advantages include rapid, flexible, and accurate characterization, the ability to differentiate between different NOM species with no sample pre-treatment required, and small sample volumes required for testing (Bridgeman et al., 2011; Hudson et al., 2007; Hur et al., 2006). Fluorescence methods can provide helpful information about the type of NOM, the difficulty of handling it, and the percentage it contains. They can also be used to explore the sources from which it is generated (Bridgeman et al., 2011).

2.1.3 Increasing NOM in Surface Water

The reasons for the increase in organic matter in water are multifaceted, with seasonal changes in the environment and temperature being key influences (Thurman, 2012). It has been found that DOC levels in water are significantly higher in the fall and winter compared to spring and summer due to increased leaf litter and other biological activity [44](Sharp et al., 2006). During the same season, the growth of DOM in the water also varied with temperature. The main reason is that biological activity becomes more frequent as temperatures rise (Matilainen et al., 2010; Xiao et al., 2020). Not only that but there is also a correlation between the amount of organic matter in drinking water sources and rainfall (Prasad et al., 2020b). According to the study, the content of dissolved organic matter in the same water source increased by 1.7 and 2.0 times in a short period after two rainfalls compared to the previous period (McDonough et al., 2020). This study also found that the composition of the organic matter in the water changes after a significant amount of precipitation. The amount of aromatic organic matter in the water was significantly higher after precipitation (McDonough et al., 2020). Changes in the content of dissolved substances in water are influenced by various factors, among which the influence of climate is relatively significant.

Moreover, in recent years, the effects of climate change have been more prominent worldwide, bringing with it a variety of climate problems not limited to rising temperatures (Houghton, 2005). According to data from eastern China, the linear trend in average

summer rainfall anomalies across the regions studied in this research has been +7.5% per decade since 50 years ago, as global warming trends have become evident (Gong & Wang, 2000). Precipitation is also becoming more variable with increasing temperatures; worse, its unpredictability is increasing (Kerr, 2007). Such uncertainty is exacerbated by the frequency of extreme precipitation events, which increases the global risk of flooding (Yoo et al., 2005).

Due to climate change and the close correlation between rainfall and NOM content in water, in general, the content of organic matter in water has shown an increasing trend in recent years (Kerr, 2007; Matilainen et al., 2010; McDonough et al., 2020). Significant increases in NOM levels in surface water sources have been found in Norwegian studies over the past decade, and the same observations have been reported from several sites in Europe and North America (Eikebrokk et al., 2004). It was found that DOC data from surface water sources showed a decade-long trend of annual increases in Nova Scotia, which directly led to adding more coagulants in the coagulation process during water treatment (Anderson et al., 2023).

2.1.4 NOM Associated Hazards

The effects of more NOM are mainly seen in the increase in the number of chemical reagents needed to treat the water and the difficulty of filtration (Anderson, DeMont, et al., 2023). Due to the increased dissolved organic matter in the water, higher doses of coagulants are added to the coagulation process to ensure uniformity of coagulation and

the water's usability (Edzwald, 1993). The filtration process also has seriously challenged the system's effectiveness due to the increase in difficult-to-filter substances in the water body (DeMont et al., 2021). At the same time, there has been an increase in the presence of metals such as iron and aluminum in surface water (Neal et al., 2008) due to the increase in coagulant doses. Furthermore, the increase in disinfection by-products (DBP) during chlorine disinfection of treated water due to the increase in organic matter is an even more severe problem and one of the primary considerations of this research (Anderson et al., 2023).

2.1.4.1 DBPs

DBPs are an unavoidable problem in water treatment process, mainly because the organic matter in the water reacts with chlorine used for disinfection and produces various by-products (Srivastav et al., 2020). The first DBPs found in the water were trihalomethanes (THMs) in sanitized swimming pools (Rook, 1972). THMs have been the most important of the DBPs that have been studied and have been considered the DBP that accounts for the most significant percentage of drinking water in relative terms (Boorman, 1999). THMs are one of two groups of DBPs for which the Guidelines for Canadian Drinking Water Quality have a legal restriction; the other is haloacetic acids (HAAs) (Canada, 2014). The maximum acceptable concentration (MAC) for THMs and HAAs are 100 ug/L and 80 ug/L, respectively (Canada, 2014). At the same time, THMs and HAAs are composed of many chemicals and not all disinfection byproducts are regulated, but their presence

can still threaten human health (Boorman, 1999). Table 2-2 lists the primary compounds detected so far for reference.

Table 2-2 Chemistry of DBPs Formation (Singer, 1994)

Class of DBP	Chemical Names
Trihalomethanes (THMs)	Chloroform Bromodichloromethane Dibromochloromethane Bromoform
Haloacetic acids (HAAs)	Monochloroacetic acid Dichloroacetic acid Trichloroacetic acid Monobromoacetic acid Dibromoaeetic acid Tribromoacetic acid Bromochloroacetic acid Bromodichloroacetic acid Dibromochloroacetic acid
Haloacetonitriles (HANs)	Dichloroacetonitrile Trichloroacetonitrile Dibromoacetonitrile Tribromoacetonitrile Bromochloroacetonitrile
Cyanogen halides	Cyanogen chloride Cyanogen bromide
Halopicrins	Chloropicrin Bromopicrin
MX	3-chloro-4-(dichloromethyl)-5-hydroxy-2 (5H)-furanone

2.2 Existing Techniques for Treating NOM and Limitations

2.2.1 Coagulation

Coagulation is the most common method for removing NOM in drinking water treatment (Matilainen et al., 2010). Coagulation is a process in which small soluble particles in water react with a coagulant to produce microparticles, thereby utilizing the decrease in the repulsive potential of the colloidal bilayer. During the flocculation stage, these microparticles collide, forming larger flocs that become easily separable (Budd et al., 2004). When NOM increases in water, enhanced coagulation is the most direct way to achieve better removal of organic matter by increasing the amount of coagulant.

Aluminum is the most common coagulant in water and wastewater treatment (Matilainen et al., 2010). Aluminum salts are generally effective in removing a wide range of impurities from water, including colloidal particles and dissolved organic matter (Duan & Gregory, 2003). The most used aluminum-based coagulant is alum ($Al_2(SO_4)_3$), and other coagulants include aluminum chloride ($AlCl_3$), poly-aluminum-chloride (PACl) etc.(Chow et al., 2009), which is widely used in drinking water treatment in Canada due to its low cost and good results (Anderson et al., 2023). Using alum at low temperatures or lower pH may result in higher levels of aluminum remaining in the finished water, which poses a health hazard or causes other problems in the distribution system, such as spontaneous flocculation. This situation can be avoided by controlling the pH, but it can also impact turbidity and NOM removal.(Matsukawa et al., 2006). Also, if there is too much NOM in the water, more aluminum coagulant is needed to help complete the

removal. However, too much aluminum has been shown in studies to have the potential to cause Alzheimer's disease (Flaten, 2001). Therefore, using alum may need to be carefully considered in some cases (Matsukawa et al., 2006).

In order not to excessively increase the use of aluminum to treat NOM, PACl has also been widely used as a more efficient coagulant (Matilainen et al., 2010b). PACl is made from partially neutralized (pre-hydrolyzed) aluminum chloride in an increased, highly charged, moderately molar mass hydrolyzed species (Dongsheng et al., 2006; Yu et al., 2007). The advantages are that it is not very demanding in temperature and pH compared to alum salts and does not require much natural alkalinity to operate efficiently because it has basicity. In many cases, the ability to remove NOM is greater than alum and requires lower dosages, leaving less aluminum in the treated water (Levchuk et al., 2018; Matilainen et al., 2010; Tang et al., 2015; Yu et al., 2007). However, PACl as a coagulant has its apparent limitations. The coagulation effect is significantly affected by the type of species hydrolyzed by the coagulant. Besides it is relatively expensive to use compared to Alum. (Dongsheng et al., 2006; Yu et al., 2007).

In addition to these two common coagulants, new types of coagulants such as iron coagulants, aluminum- and iron-based polymeric flocculants combined with polyciliate, inorganic salts and polyelectrolytes, etc., are constantly being developed and utilized in water treatment (Matilainen et al., 2010). However, these coagulants have their limitations or very high price costs, this gives it significant limitations in practical use (Matilainen et al., 2010).

2.2.2 Adsorption by Active Carbon

Adsorption technology is one of the standard and effective methods for NOM removal in water treatment (Korotta-Gamage & Sathasivan, 2017). Due to its unique, highly porous structure and efficient adsorption properties, activated carbon is widely used in this field (Satya Sai et al., 1997). Activated carbon is characterized by its very high surface area, porous structure, and unique surface chemistry, which enable it to effectively adsorb and immobilize various organic and inorganic substances (Moreno-Castilla, 2004). The adsorption capacity of activated carbon is influenced by its surface area, pore structure and surface chemistry. A larger surface area provides more adsorption sites. At the same time, the pore structure determines the selectivity and diffusion rate of the adsorbent, and the surface chemistry influences the affinity between the adsorbent and the adsorbate (Newcombe & Drikas, 1997; Xing et al., 2008).

In drinking water treatment, there are two primary forms of activated carbon: granular activated carbon (GAC) and powdered activated carbon (PAC) (Korotta-Gamage & Sathasivan, 2017). Granular activated carbon is typically used in continuous flow treatment systems, which continuously removes impurities from the water. Conversely, powdered activated carbon is often used when rapid treatment and effective removal of contaminants quickly is required, such as emergency treatment. Both have their unique advantages and applications in different treatment scenarios.

Activated carbon has an excellent effect on NOM removal (Newcombe & Drikas, 1997). However, it has its limitations. The main limitation is that it loses its absorption capacity

over time and decreases porosity (Ghosh et al., 1999). One of the main reasons for the decrease in adsorption capacity is the occupation of adsorption sites by absorbed organic matter and the ability of contaminants to form complexes with organic carbon and change its physical, chemical and transport properties (Ghosh et al., 1999; Quinlivan et al., 2005; Woo et al., 1997). Once activated carbon loses its absorptive capacity, it cannot recover independently and needs to be artificially restored (Newcombe & Drikas, 1997). Currently, there are methods such as catalytic processes, extractive regeneration, reactive regeneration, etc. Regardless of the method, there is a certain amount of secondary pollution and a large amount of energy consumption, an unavoidable limitation of using activated carbon (El Gamal et al., 2018; Sheintuch & Matatov-Meytal, 1999).

2.3 Advanced Oxidation Process

Advanced Oxidation Processes (AOPs) all share a standard chemical signature that enables the use of a variety of highly reactive with highly oxidizing free radicals to break down complex organic compounds, resulting in the degradation and mineralization of less reactive contaminants (Andreozzi et al., 1999). AOPs are one of the most cutting-edge drinking water purification and disinfection technologies, and due to their extensive range of adaptations and the absence of secondary contamination, they have yielded promising results (Jarvis et al., 2008; Toor & Mohseni, 2007). Although, in many cases, AOPs have not been detected to reduce the total amount of NOM ultimately, several studies have shown that AOPs are effective in degrading specific large molecules of NOM into smaller ones and slowing down the formation of DBPs (Matilainen & Sillanpää, 2010).

This chapter will introduce several common AOPs, including those used in this paper. Finally, a description and identification method of free radicals they produce and the reaction mechanisms will be given, including examples of existing methods and limitations.

2.3.1 Ozone-Based Advanced Oxidation Technologies.

As one of the most traditional AOP processes, the ozone process is characterized by its direct reaction and extremely high efficiency (Parsons, 2004). Due to its high efficiency and ability to comprehensively treat organic matter, experiments have demonstrated its feasibility in treating water bodies on a large scale. The main ozone-based advanced

oxidation process classifications are O_3/UV, O_3/H_2O_2, O_3/Homogeneous catalyst and direct ozone oxidation (Rekhate & Srivastava, 2020). The ozone process has many applications in drinking water and wastewater treatment. The first prerequisite for using ozone AOP is the need to make ozone, which requires oxygen to be made by electrical energy in an ozone-making apparatus (Rakness et al., 1996), the efficiency of which generally depends on the power level of the electrical power, whose reaction formula is shown in Equation 2-2 (Rekhate & Srivastava, 2020; Tichonovas et al., 2017).

Equation 2-2 Ozone Generation Pathway

$$O_2 + eletric\ spak \rightarrow 2O \cdot O_2 + O \cdot \rightarrow O_3$$

However, the ozone combined with the UV process requires relatively high power costs. Therefore, it is more reasonable to use ozone directly to treat drinking water if it is used on a large scale in production. Experiments have shown that ozone can also effectively reduce organic matter in water, thereby reducing DBPs (S. MacIsaac, 2021). However, the reason for the reduction is a direct reduction of TOC and the decomposition of large organic molecules into small, easily degradable molecules remains to be demonstrated(Parsons, 2004; Rekhate & Srivastava, 2020; Tichonovas et al., 2017). The formula for the production of hydroxyl radicals by the direct reaction of ozone in water is shown in Equation 3-3 (Rekhate & Srivastava, 2020).

Equation 2-3 Ozone advanced oxidation reaction pathway

$$O_3 + H_2O \rightarrow H_2O_2 + O_2$$

$$H_2O_2 \rightarrow 2\,OH\cdot$$

2.3.2 UV/H_2O_2 Advanced Oxidation Technologies

H_2O_2-based advanced oxidation has a long history of degrading target organic compounds in natural water matrices, and the conclusions of many studies have demonstrated its effectiveness and potential for practical application (Beltrán et al., 1993; Rosenfeldt et al., 2006). A few of the more common hydrogen peroxide-related advanced oxidation techniques are UV/Fe^{2+}/H_2O_2, UV/H_2O_2, Fe^{2+}/H_2O_2, and H_2O_2/O_3 (Lamsal et al., 2011; S. MacIsaac, 2021; Xu et al., 2009). Overall, H_2O_2-based AOPs have a more direct chemical pathway for the generation of hydroxyl radicals, with one mole of hydrogen peroxide splitting into 2 moles of hydroxyl radicals in an energy-catalyzed reaction equation shown in 2-1 (S. MacIsaac, 2021).

Equation 2-1 H_2O_2-Based Advanced Oxidation Pathway.

$$H_2O_2 \xrightarrow{h\nu} 2OH\cdot$$

$$2\,(H_2O_2 + OH\cdot) \rightarrow H_2O + HO_2\cdot$$

$$2HO_2\cdot \rightarrow H_2O_2 + O_2$$

Among these, UV/H_2O_2 AOPs have been widely investigated in drinking water treatment and have great potential (Toor & Mohseni, 2007). It was found that this technology has great potential in drinking water treating NOM along with many of the same micropollutants as pharmaceutical products (Jung et al., 2012; Muruganandham &

Swaminathan, 2004). In addition, UV/H_2O_2 technology can be applied on a large scale to remove micropollutants and organics at a much lower cost than other advanced oxidation technologies (Miralles-Cuevas et al., 2017).

Studies have found that UV/H_2O_2 AOPs can reduce the formation of DBPs in drinking water in two ways; they also found that after this treatment at high doses of UV as well as hydrogen peroxide can completely oxidize or mineralize NOM and reduce the TOC content (Parsons, 2004; Sundstrom et al., 1986). In a UK-based study, a UV/H2O2 AOP was highly effective in directly degrading not only UV254 but also DOC. 254nm UV-C LP was used as the light source, and the degradation of DOC in natural water with a raw DOC of 17.4mg/L was achieved at a dose of 22,000mJ/cm^2 of UV radiation in combination with 2mM H_2O_2. The degradation rate of DOC in natural water with original DOC of 17.4 mg/L reached 74% (Goslan et al., 2006). Other studies have found that UV-H2O2 intermediate treatment partially oxidizes NOM and its sizeable molecular weight constituents to smaller, more biodegradable substances, thereby reducing the production of DBPs (Matilainen & Sillanpää, 2010; Toor & Mohseni, 2007). Recently, however, experiments on drinking water sources found that advanced oxidation by UV mercury lamps in combination with hydrogen peroxide not only did not reduce the generation of DBPs but also led to an increase in the content of THMs (S. MacIsaac, 2021). The results of experiments on this technology regarding drinking water have been contradictory in many studies. Therefore, more research is needed on the UV-H2O2 advanced oxidation of organic matter to determine its effects on water bodies.

2.3.3 Chlorine-Based Advanced Oxidation Technologies

Chlorine-based AOPs are one of the emerging technologies for water treatment AOPs since chlorine is the chemical used for disinfection in the final step of water treatment (Gil et al., 2019). For this reason and because of the availability of chlorine disinfection tanks, Cl_2-AOP is also a good choice for the use of AOP in current treatment plants, as it can be easily retrofitted into existing drinking water treatment plants, especially after installation and filtration, so that upgrades can be accomplished in the existing water treatment plant (Lamsal et al., 2011; S. MacIsaac, 2021). Chlorine-based advanced oxidation is mainly accomplished by optically catalyzed HClO, where UV is the primary excitation (Cheng et al., 2020). Moreover, due to the instability of chlorine in water, the mechanism regarding its reaction with UV of different wavelengths and the products of advanced oxidation is also different (Wang et al., 2016). Moreover, according to some studies, the chlorine-based advanced oxidation reaction under UV radiation below 400 nm, which is also the principle of the UV- Cl_2 reaction in this study, is shown in Equation 2-4 (Liu et al., 2020).

Equation 2-4 UV/Chlorine advanced oxidation reaction pathway

$$HOCl \leftrightarrow H^+ + OCl^- \ (pK_a = 7.5)$$

$$HOCl \xrightarrow{UV} OH\cdot + Cl\cdot$$

$$OCl^- \xrightarrow{UV} O^-\cdot + Cl\cdot$$

$$O^-\cdot + H_2O \rightarrow OH\cdot + OH^-$$

Based on these equations, chlorine and hydroxyl radicals are the leading reactive radicals for the advanced oxidation of chlorine radicals. However, many different radicals have been found in the literature to be involved in chlorine-based reactions, and the differences in radicals may come from a combination of the pH of the reaction, different wavelengths, and different reacting substances.

It has been demonstrated that chlorine-based AOP is more effective than H_2O_2-based AOP in reducing fluorescence intensity and UV_{254} in water treatment experiments(Sgroi et al., 2021). It is also more effective in treating complicated drug compounds such as antibiotics than hydrogen peroxide and ozone (Sgroi et al., 2021; Farzanehsa et al., 2023; Toor & Mohseni, 2007). While UV/chlorine experiments appear more advantageous for UV_{254} reduction, chlorine-related advanced oxidation experiments have a greater risk of producing more DBPs due to adding additional chlorine reagents (Yin, Zhong, et al., 2018). Also, due to the change in chlorines form in the water by UV, the disinfection by-products produced are uncertain and may even produce new types of by-products that cannot be detected (Tian et al., 2020). Therefore, more experiments are needed to measure the risk and value of chlorine-based advanced oxidation to determine whether it is feasible for practical large-scale use.

2.3.4 Determination Method of Advanced Oxidizing Radicals

Determining reactive radicals is an important step to find the optimal conditions for advanced oxidation (Jarvis et al., 2008; Rekhate & Srivastava, 2020; Wang et al., 2016).

The most mature technique in free radicals is the use of pCBA for the determination of OH-; the maturity of this technique is reflected in the stability of pCBA under non-radical interference, which is challenging to be interfered with by other factors (Rosenfeldt et al., 2006). For this reason, it is possible to measure the free radicals produced, allowing the strength of the reaction and the principle to be determined (Elovitz & Von Gunten, 1999). In an idealized or pure water system, pCBA is degraded by ozone. Therefore, it is not easy to use pCBA to identify free radicals in ozone experiments (Pi et al., 2005).

As previously discussed, for chlorine-related reactions, the reaction is a combination of different radicals (not only hydroxyl radicals), so pCBA is not the best choice in this case (Farzanehsa et al., n.d.; Rosenfeldt et al., 2006; Sgroi et al., 2021). It has been shown in several studies that the use of nitrobenzene in chlorine-based reactions allows the extraction of the reactive fraction of OH • alone (Liu et al., 2020; Sun et al., 2016). Moreover, the separation of Cl • can be measured by benzoic acid as an indicator to determine the proportion of this radical in the reaction. The equations for these two reactions are shown in Equations 2-4 (Liu et al., 2020; Sun et al., 2016; Xu et al., 2009). However, since the method has not been fully developed, various other factors can affect the concentration of benzoic acid. It is also possible that there are many more free radicals than those produced in the chlorine-based reaction. Therefore, it is necessary to continue researching this issue.

Equation 2-4 Calculation of OH • and Cl • by nitrobenzene and benzoic acid

$$\int [OH \cdot]_t dt = \frac{\ln([NB]_t/[NB]_0)}{k_{NB,OH\cdot}}$$

$$\int [Cl \cdot]_t dt = \frac{\ln([BA]_t/[BA]_0) - k_{BA,OH\cdot} \int [OH \cdot]_t dt}{k_{BA,Cl\cdot}}$$

2.4 UV Technology for Water Treatment

Ultraviolet (UV) technology has been widely used in the field of water and wastewater treatment for decades, primarily for sterilization and disinfection and, more recently, for advanced oxidation with the treatment of difficult-to-degrade organics in water (Sarathy & Mohseni, 2006; Song et al., 2016; W. Yang et al., 2014, 2014). In contrast to traditional chemical disinfection methods, UV disinfection produces regulated DBPs and does not require adding any chemicals (Meulemans, 1987; Sommer et al., 1998). In treating organics, it is also characterized by reduced chemical additions, high efficiency, and universality (W. Yang et al., 2014).

The UV and visible spectra are shown in Figure 2-1, showing UV wavelengths from 100 nm to 400 nm are UV (S. MacIsaac, 2021). Ultraviolet light can be divided into four categories according to wavelength: UV-A (315~400nm), UV-B (280~315nm), UV-C (200~280nm) and vacuum UV (100~200nm) (Förster, 2004). The best and most promising research for disinfection and advanced oxidation applications is currently UV-C, which will be this paper's UV wavelength of focus (Sarathy & Mohseni, 2006; Song et al., 2016).

This chapter will then analyze the traditional UV mercury lamp, the advanced UV-LED technology and the future of UV technology in water treatment technology development.

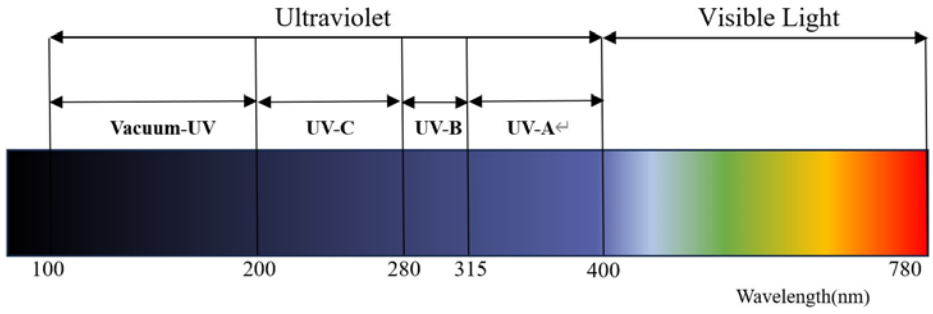

Figure 2-1 Visible light and UV spectrum

2.4.1 Mercury UV Emitters

The most common and traditional UV technology used today is UV mercury lamp technology (S. MacIsaac, 2021). UV mercury lamps are discharge lamps mainly containing mercury vapour and other gases. The main principle of operation is that when an electric current is passed through these gases, the mercury vapour produces UV light (Heikkilä et al., 2009). Generally speaking, according to the power size, UV mercury lamps are divided into medium-pressure mercury lamps (MP) and low-pressure mercury lamps (LP) (S. MacIsaac, 2021). MP is generally used as a high-level oxidizing light source to treat organic matter; low-pressure mercury lamps are used as disinfection equipment(Sarathy & Mohseni, 2006; Song et al., 2016). They have the advantage of higher power and efficient treatment capacity.

Although it can be practically used in water treatment on a large scale, UV mercury lamps have some limitations (Roback et al., 2021). First, the wavelengths of mercury lamps are diffuse, especially in low-pressure mercury lamps, and it is not possible to concentrate the energy at specific wavelengths. In addition, UV lamps need to be replaced regularly and must be disposed of properly because they contain harmful mercury (Hölz et al., 2017). They also have a relatively large equipment size, as shown in the laboratory schematic in Figure 2-2. In summary, using UV mercury lamps in aqueous environments provides a viable method of disinfection and advanced oxidation for water treatment that can be implemented on a large scale. However, its limitations, application conditions, and environmental contamination must be considered.

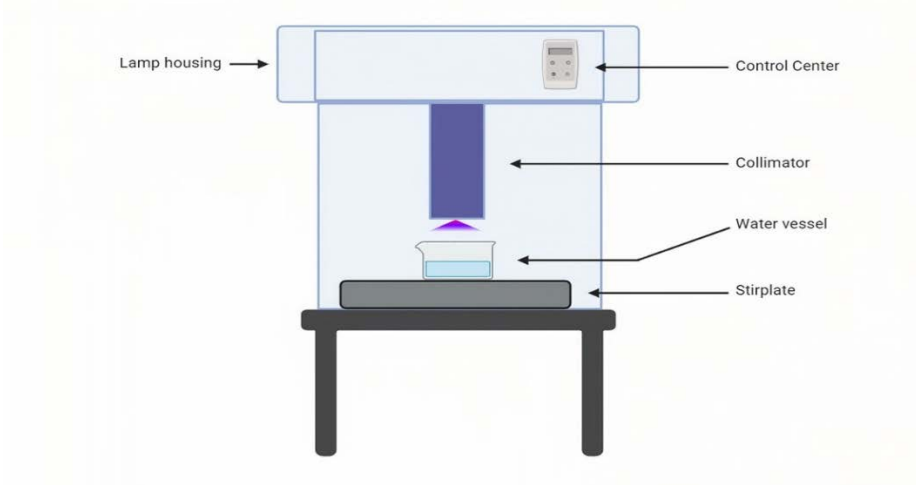

Figure 2-2 Bench-scale UV MP Set-up

2.4.2 UV Light Emitting Diode Emitters (LEDs)

As an alternative to large, toxic gas-based UV mercury lamps, compact, high-efficiency UV solid-state light sources, UV-LEDs have attracted significant interest in water

treatment in recent years (Taniyasu et al., 2006). UV-LEDs are not only environmentally friendly and energy efficient compared to traditional mercury lamps, but more importantly, they have a long service life, are compact and can be easily adapted to various designs (Beck et al., 2017; Song et al., 2016).

Another advantage of LEDs in water treatment is that their wavelengths are more concentrated and selectable. This is especially true in disinfection, where many studies have found that applying different wavelengths of UV light makes a difference in killing microorganisms (Song et al., 2016). Moreover, different UV wavelengths have different killing efficiencies for different microorganisms (Muramoto et al., 2014). Regarding disinfection, UV-LEDs demonstrate a much higher potential and efficiency than mercury lamps(S. A. MacIsaac et al., 2023).

Meanwhile, research in UV-LEDs in advanced oxidation is not as widespread as sterilization. Most of the studies have focused on studying wastewater treatment and the degradation of antibiotics (Yin et al., 2020; Yin, Ling, et al., 2018). Notably, these studies have found that the amount of free radicals produced by the same UV radiation dose under certain conditions is not inferior to that of UV mercury lamps (W. Yang et al., 2014; Yin et al., 2020; Yin, Ling, et al., 2018).

In recent years, research has found that UV-LEDs have also been beneficial for full-scale drinking water disinfection treatment (Jarvis et al., 2019). This study is fascinating to fill

the experimental gap of UV-LEDs for the advanced oxidation part of natural drinking water.

2.4.3 Future Prospects for UV Technologies

As our planet witnesses an escalating demand for untainted drinking water, UV technology is emerging as a cornerstone in water treatment. Its swift, residue-less disinfection modality prowess is commendable; UV technology also plays a seminal role in advanced oxidation processes. This opens innovative avenues for tackling and eliminating tenacious organic contaminants that often elude conventional treatments. This breakthrough promises heightened efficiency and fosters a more sustainable and cost-effective approach to water purification. Given its myriad advantages, UV-LED technology will become integral to large-scale water treatment infrastructures globally.

Chapter 3: Material and Methods

3.1 Water Source and Water Characteristics

Pockwock Lake, a primary drinking water source in Halifax, was selected as the subject of this study. As a representative drinking water lake in Nova Scotia, this water source is characterized by low alkalinity (<5 mg/L $CaCO_3$) and low pH (<6) (Stoddart & Gagnon, 2015). In recent years, there has been an increasing trend of elevated NOM levels in the water of Pockwock Lake and associated water quality problems (Anderson et al., 2023). To simulate the treatment process of specific drinking water, the water body in the Pilot Plant of J.D. Kline Water Supply Plant, which takes water directly from Pockwock Lake, was selected as the experimental object.

3.1.1 J.D. Kline Water Supply Plant and Pilot Plant

The J. Douglas Kline Water Supply Plan (JDKWSP) is the primary drinking water supply plant in the Halifax area. The plant draws raw water directly from Pockwock Lake, where it undergoes treatment steps, including pre-screening, oxidation, pre-chlorination (only in algal risk conditions), coagulation and flocculation to remove particulates, direct dual media (2-feet anthracite and 1-foot sand) filtration, and finally chlorine disinfection before entering the distribution system. The increasing trend in Natural Organic Matter (NOM) levels in Pockwock Lake water throughout the 21st century is clearly discernible, as demonstrated by the rising trends in DOC and color averages depicted over consecutive years in Figure 3-1.

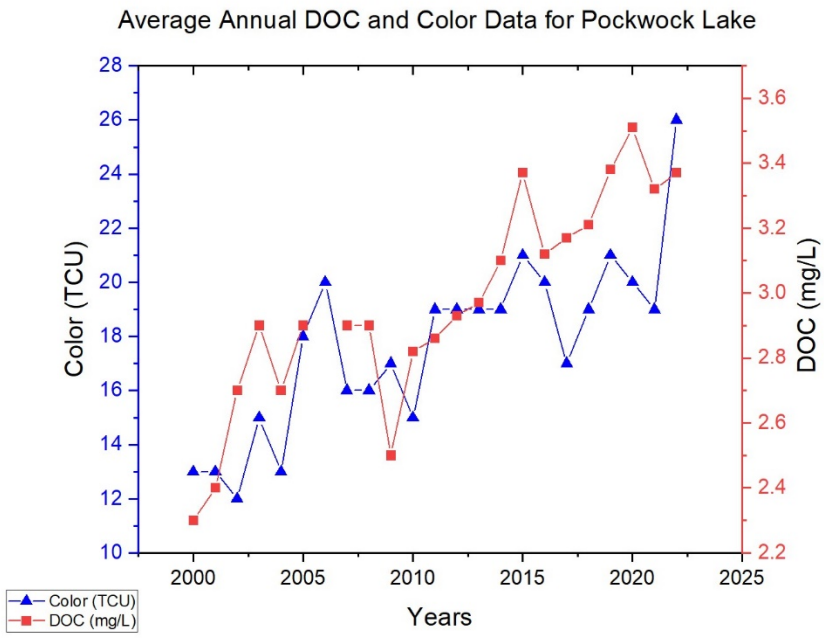

Figure 3-1 Historical average annual DOC and color for Pockwock Lake (Anderson et al., 2023)

The coagulant added during the coagulation process is alum, and the amount added is determined by the amount of organic matter detected in the water. Similarly, in the final disinfection process, the amount of chlorine added varies with residual in the distribution system; the residual of the chlorine is related to the organic matter in the water. Water entering the plant is first pre-oxidized with potassium permanganate at a rate of 0.15 mg/L, and the pH is adjusted to 9.6-10 using lime. JDKWSP primarily uses aluminum sulfate as the coagulant, at an average dosage of about 20 mg/L (Anderson et al., 2023). The water is then coagulated with a cationic polymer to improve coagulation and flocculation properties and to increase the flocculation time. Subsequently, cationic polymers are added to improve coagulation and flocculation properties and to reduce the flocculation time. After flocculation there is no clarification stage, and the water goes directly to filtration.

Water containing flocculants enters a dual media anthracite and sand filter. Before entering the water distribution system, it is chlorinated and disinfected. The chlorine dosage in the water treatment plant is adjusted according to the concentration of organic matter in the filtered water, rather than being kept constant. In recent years, there has been an upward trend in the concentrations of organic matter detected in the raw water, and an increase in DOC of about one mg/L has been found in the natural moisture. This places higher demands on water treatment processing with the need for more aluminum and chlorine to treat these issues (Anderson et al., 2017).

3.1.1.1 Pilot Plant

Within the J.D. Kline Water Supply Plant, a Pilot Plant was established for experimental research and to explore improvement and innovation programs. The raw water is divided into two treatment trains in the Pilot Plant. The treatment process of the first train is the same as that of the J.D. Kline Water Supply Plant and is used as a reference group to compare the second train. The second train is akin to the first one, with the difference of a sedimentation step before filtration. The second train was chosen for the experiment, in which the processing flow is shown in Figure 3-2.

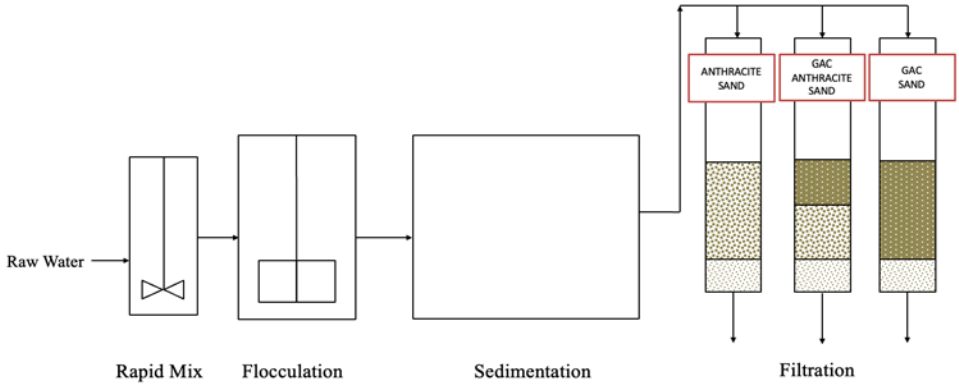

Figure 3-2 JDKWSP pilot plant treatment process schematic

In this experiment, the second train was selected as the experimental water sampling point, and its general processing flow is shown in Figure 3.1. It is worth noting that this process has three different filtration systems. The first filtration system is identical to that of the Water Supply Plant, 2-feet anthracite and 1-foot sand, referred to as the Ant/Sand filtration system. The second filtration system replaced the top foot of anthracite with GAC, which helped absorb some of the organic matter and was called GAC/Ant/Sand. The third filtration system replaced both feet of anthracite with GAC, forming the GAC/Sand filtration system. In this experiment, Sedimentation, Ant/Sand, and GAC/Sand were selected as sampling points to measure the effect of different locations in the process and other filtration systems on advanced oxidation to determine representative water samples (Anderson et al., 2023).

3.2 Analytical Methods

The main parameters measured in this experiment before and after treatment were TOC/DOC, UV Scan, SUVA, free chlorine, pH, THMFP, HAAFP, and FEEM. The

measurement and essential preservation of the experimental water samples follow the standard testing procedures, and the reference book used was *The 19th Edition of Standard Methods for the Examination of Water and Wastewater* (Clesceri et al., 1996).

3.2.1 TOC/DOC

To measure TOC, water samples were collected and filled in 40 mL glass vials, fixed with four drops of phosphoric acid (85%), sealed with a tinfoil cover, and stored in a refrigerator at approximately 4 ºC. DOC testing was performed similarly to TOC, except the water samples were filtered through a 0.45 μm membrane before measurement. The TOC/DOC of water samples were analyzed in a TOC-V CPH analyzer equipped with a Shimadzu ASI0-V autosampler and a catalytic combustion oxidation non-dispersive infrared detector (NDIR). This detector has a detection limit of 0.08 mg/L, meaning the detectable TOC/DOC concentration must be higher than 0.08 mg/L.

3.2.2 UV-Vis Scan & SUVA

For UV-Vis scan measurements, a HACH DR/6000 UV/Visible spectrophotometer was used with a zero-point calibration in the wavelength range of 190 nm to 900 nm, using Milli-Q water for calibration. The water sample was removed for cleaning and filling the 1-cm glass cell for UV-Vis scan measurements. It is important to note that all test water samples must be filtered through a 0.45um filter membrane.

SUVA is the ratio of the UV absorption coefficient of dissolved organic matter to the concentration of DOC. It is used to assess the UV absorbance properties of dissolved organic matter in water samples, mainly to provide some information on the origin and degradation of organic matter. The specific wavelength selected in this experiment was 254 nm, and the absorbance of the water sample at 254 nm can be found in the data of the UV scan. The measured absorbance coefficient at 254nm UV was divided by the corresponding DOC concentration to calculate the SUVA value. Usually, SUVA is expressed in units of L/mg • m

.

3.2.3 Free Chlorine Measurement

This study determined free chlorine in the chemical solution's configuration and the solution's decision after its reaction. On this DR6000 HACH spectrophotometer, the F&T chlorine measurement method was selected with an upper limit of 2 mg/L. A proportional dilution was required if the free chlorine in the water sample exceeded 2 mg/L. Method calibration was performed using Milli-Q water. A DBP free chlorine reagent containing disodium hydrochlorate hydrochloride (EDTA), sodium phosphate dibasic, and N, N-diethyl-p-phenylenediamine hydrochloride was used for each free chlorine measurement. After shaking 10 mL of the measurement sample with a bag of reagent powder in a 10 ml standard measuring dish, the reaction was waited for three minutes before completing the test.

3.2.3 Uniform Formation Potential (UFC) Test

The UFC test provides a stable and representative chlorinated disinfection by-product formation condition. For the UFC test, chlorination conditions were selected to include a pH of 8 ± 0.2, an incubation temperature of 24 ± 1°C, an incubation time of 24 ± 1 h, and a 24 h free chlorine residual of 1.0 ± 0.4 mg/L. Different chlorine disinfection concentrations were formed by adjusting the water samples to pH eight and titrating them with a chlorine solution of adjusted pH 8, stored in 130 ml amber bottles. The bottles were sealed and kept from light for 24 hours at about 24 °C. After 24 hours, the free chlorine concentration in the water was measured to determine the concentration of chlorine that needed to be added after the disinfection reaction. *Standard Methods for the Examination of Water and Wastewater* was used as a reference for its operation and the specific experimental procedures for cleaning (Bridgewater et al., 2017).

3.2.4 THMFP and HAAFP

Before measuring THMFP and HAAFP, 50 g/L ammonium chloride solution, two drops of 8 g/L sodium sulphite solution, and three drops of 0.1 N hydrochloric acid for the collection of THM samples, one drop of 50 g/L ammonium chloride solution, two drops of 8 g/L sodium sulphite solution, and three drops of 0.1N hydrochloric acid were added to each pre-washed glass vial. Then, THM samples were collected in these glass vials under air-free conditions. HAA samples were kept in baked 23 ml glass vials in an air-free manner with one drop of 50 g/L ammonium chloride solution.

The THM in the sample is extracted by liquid-liquid extraction gas chromatography with THMs and chlorinated organic solvents and then tested. The primary analysis of THMFP in a fixed finished 23 ml THM sample vial was performed using a Thermo Scientific Trace 1310 gas chromatograph equipped with an AI/AS 1310 autosampler. One uL of THM extract was injected into a Thermo Scientific Split/Splitless Inert 4 mm swallow neck injection tube with glass wool into the GC at a separation flow rate of 18 mL/min and a separation ratio of 15%, where the inlet temperature was 220 degrees C. A Thermo Scientific TG-5SILMS 30m x 0.25 mm x 0.25 μm column was used for this experiment, and ultra-high purity helium (99.999%) was selected as the carrying gas. The investigation was started with the oven temperature set at 35°C and held for 3.00 min. We then increased the temperature to 80 °C at 60.0 °C/min without any hold time. Next, we continued to ramp up to 85°C at a rate of 1.0°C per minute, again without any hold time. We then rapidly ramped up to 180°C at a final speed of 125.0°C/min, again with no hold time. The total run time for each sample was 9.510 minutes. THM samples were run in this experiment at a constant 1.2 mL/min flow rate. We used an electron capture detector (ECD) for THM detection, and the data acquisition rate was set to 10 H detector temperature to 320°C. The pulse amplitude was set to 50 V, the pulse width to 1.0 μs, and the reference current to 0.5 nA.

The present experiment differs from conventional experiments in that HAAFP was determined from liquid chromatography-mass spectrometry LC/MS. Unlike the traditional method of analyzing HAAFP using meteorological chromatography, this method does not require extraction or filtration of the immobilized sample. The LC/MS assay for HAA used

in this paper is based on the LCMS reference employed by an Agilent 1260 Infinity LC and an Agilent 6460 Triple Quad LC/MS device (Daniel & Technologies, n.d.).

3.2.5 Fluorescence Excitation Emission Matrix (FEEM)

All FEEM samples for this experiment were filtered through 0.45μm filter membranes, loaded into 1cm-glass cells, and measured by Aqualog-UV-800. This instrument's excitation spectra (EX) ranged from 239 nm to 800 nm, and the emission spectra (E) ranged from 246.129 nm to 824.884 nm. The operating system Aqualog V4.3 was selected, the bandwidth resolution was set to 3 nm in both the excitation and emission spectra in the operating system, and the integration time was 1 second. Milli-Q water was used as a blank sample, and the test sample was started after confirming that the system passed the self-test. After the samples were tested, the data were all exported as CSV. Table 3-1 and Table 3-2 summarize the fluorescence profile of each NOM fraction (Coble et al., 2014). All the mapping methods for the FRI in this thesis using FEEM shining app made for the lab.

Table 3-1 Excitation (EX) and emission (EM) wavelength ranges of five regions (Chen et al., 2003)

Region	Characteristics	EX (nm)	EM (nm)
Region I	Aromatic Protein I	200-250	200-330
Region II	Aromatic Protein II	200-250	330-380
Region III	Fulvic acid-like materials	200-250	380-550
Region IV	Soluble microbial materials	250-340	200-380
Region V	Humic acid-like materials	250-400	380-550

Table 3-2 Defined regions for observing fluorescence peaks in excitation (EX) and emission (EM) spectra of organic matter in water (Coble et al., 2014)

Component	EX (nm)	EM (nm)
Humic-like(A)	250-260	380-480
Tyrosine-like(B)	270-280	300-320
Humic-like(C)	330-350	420-480
Marine humic-like(M)	310-320	380-420
Tryptophan-like(T)	270-280	320-350

3.2.6 4-chlorobenzene Acid (pCBA) Analysis

4-chlorobenzoic Acid (pCBA) is a joint advanced oxidation probe compound commonly used primarily as an assay for the generation of hydroxyl radicals during advanced oxidation processes related to hydrogen peroxide (Lanzarini-Lopes et al., 2017). This experiment used 99% 4-chlorobenzoic Acid from Simga-Aldrich as the raw material. Due to the nature of pCBA, 250 μmol/L(S. MacIsaac, 2021; Rosenfeldt et al., 2006) stock solution was prepared under heating conditions in a water bath and stored at 4 degrees Celsius in a refrigerator protected from light. Subsequently, 10μmol/L, 20μmol/L, 30μmol/L, 40μmol/L, and 50μmol/L of the test sample stock were diluted before formal experiments were required.

The concentration of pCBA was determined by high-performance liquid chromatography (HPLC). The HPLC used in this experiment was a PerkinElmer Series 200 HPLC system consisting of an Autosampler, Pump, UV/VIS Detector, and a Data Handling System. The autosampler syringe was cleaned with a water/methanol mixture (1:4). The autosampler

syringe is cleaned with a variety of water and methanol (1:4). The mobile phase used in the cleaning pipeline is analytically pure acetonitrile, and the flow rate used is 2 ml/L. The mobile phase used in the cleaning pipeline is analytically pure acetonitrile.

The composition of the mobile phase used to determine pCBA was acetonitrile/Milli-Q water (60:40), and the set flow rate was 0.9 ml/L. The peaks were relatively stable under the conditions of this assay, and there were fewer stray peaks. The pressure change of the pump was recorded for each experiment to protect the column as well as the safe operation of the equipment, and the pressure was generally between 1350 and 1380 in the investigation. Wash samples were added between every ten measurements and were prepared with Milli-Q water.

The actual sample concentration and peak area were plotted as x and y-axis, respectively. This method measured previously configured samples of 10 to 50 μmol/L to develop a standard curve, as shown in Figure 3-3. The linearity of its standard curve has an R-squared of 0.9998 (Figure shows 1.00), presenting an excellent linearity. From this curve, the concentration of pCBA was determined by measuring the peak area of the pCBA samples with a limit of 0-50 μmol/L. The concentration of pCBA in the model was determined by measuring the peak area of the pCBA sample.

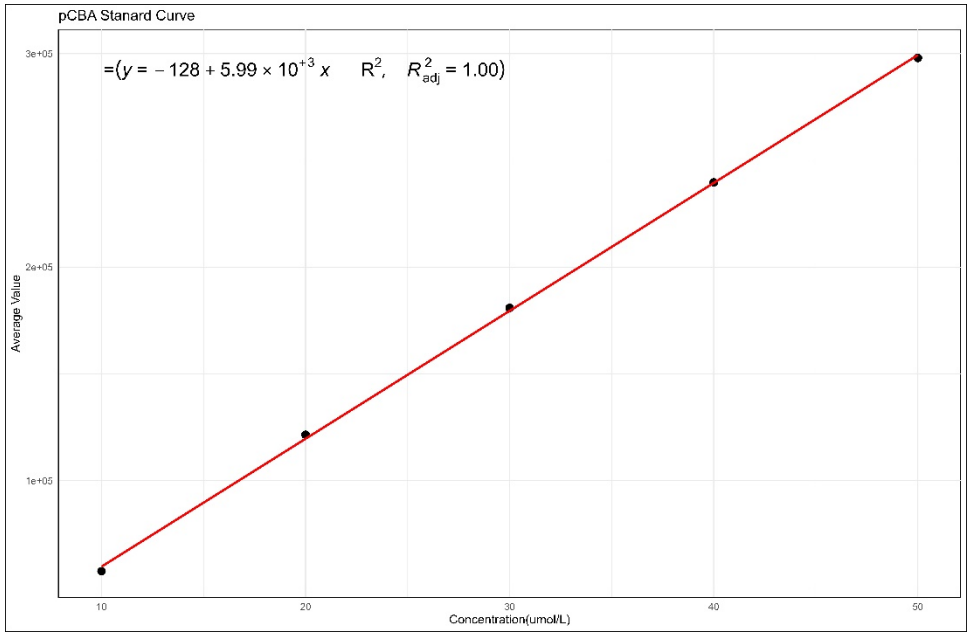

Figure 3-3 pCBA standard curve

Based on the degradation trend lines of pCBA, as k_d for those that were acted upon by the UV alone and k_{obs} for those that were reacted upon by the H_2O_2 in conjunction with the UV. Furthermore, by using the constant $k_{OH\text{-}pCBA}$ ($5\times10^{9}M^{-1}S^{-1}$) summarized in the study about the correlation between hydroxyl radicals and pCBA degradation rate, combined with Equation 4-1, Equation 4-2 it is possible to calculate the number of hydroxyl radicals produced in each reaction's response (Rosenfeldt et al., 2005, 2006).

Equation 3-1 Radicals calculation equation for only UV

$$R_{OH} = \frac{k_d}{k_{OH-pCBA}}$$

Equation 3-2 Ozone advanced oxidation reaction pathway

$$R_{OH} = \frac{k_{obs} - k_d}{k_{OH-pCBA}}$$

3.3 Advanced Oxidation Experimental Design

3.3.1 UV-related Advanced Oxidation Experimental Design

Due to technical constraints, the experiments were conducted in a laboratory setting, as in Figure 3-4, to simulate the UV-advanced oxidation process in a drinking water treatment plant. In this experiment, the UV-LEDs at 280 nm was chosen as the source of all UV light, and all UV fluence was measured and computed by Bolton and Linden's method (Bolton & Linden, 2003). In the UV advanced oxidation experiment, three different fluences of 100mJ/cm^2, 500mJ/cm^2, and 1000mJ/cm^2 were selected as low, medium, and high UV radiation doses. Compared with the previous experiments on UV-MP AOPs, an additional 500 mJ/cm^2 at 100 and 1000 mJ/cm^2 was selected to give a more comprehensive reference for practical applications (S. MacIsaac, 2021). Higher doses may be difficult to achieve in practical applications (Rosenfeldt et al., 2006; Toor & Mohseni, 2007). 100 ml of the experimental water sample was added to a 130 ml Petri dish. Due to the limitations of the single experimental volume of the samples, for subsequent experiments to determine DBPFP, multiple experiments were required to mix the water samples to complete a single determination of the data.

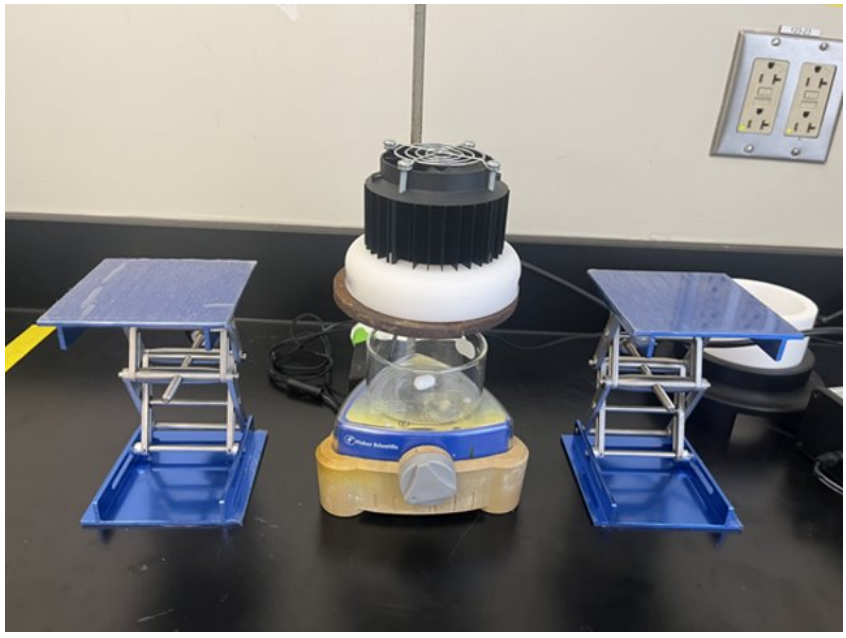

Figure 3-4 Bench-scale Advanced Oxidation System

The hydrogen peroxide and chlorine added to the water were set at 1 mg/L and 10 mg/L as low and high concentrations, respectively. Such a choice of oxidizer dose is consistent with the dose selected for previous MP AOPs experiments for comparison purposes (S. MacIsaac, 2021). The hydrogen peroxide was obtained from a stock solution of 5000 mg/L of hydrogen peroxide. Moreover, chlorine was obtained from the original configuration of 5000 mg/L free chlorine concentration of sodium hypochlorite solution. Due to the volatility of chlorine, it was necessary to recalibrate the free chlorine concentration of the solution every week of the experiment using the method mentioned in the previous section.

To analyze the reaction, and remove additional interfering factors, hydrogen peroxide and chlorine needed to be quenched immediately after the reaction was completed. The samples were quenched immediately after UV/hydrogen peroxide treatment using bovine

catalase in the laboratory, where the dose of catalase was added in excess each time to ensure complete quenching of the hydrogen peroxide. The UV/chlorine treated samples were also quenched immediately after treatment with the experimentally configured 5000 mg/L sodium sulphite solution, which was added in excess doses. After completing the quench, the water samples are stored and analyzed for various tests.

3.3.2 Ozone Advanced Oxidation Experimental Design

Similarly, the laboratory constructed this experiment to simulate advanced ozone oxidation, using an Azocon VMUS ozone generator to generate and transport ozone through the pipeline to the experimental water body, as shown in Figure 3-5. The semi-batch method was chosen to assess better the specific ozone content absorbed in the water (Mathon et al., 2017). The flow rate of the ozone generator was set to 2 L/min, and the generator's power was set to 50%. The ozone concentration in the water body is controlled by adjusting the time to 1mg/L and 10mg/L, calibrated as low and high concentrations. Because ozone is unstable in the water column, it evaporates quickly, so no additional quenching is required. Regardless, at the end of the experiment, it is usually left for 1 to 2 minutes to ensure complete evaporation. For ozone experiments, on the other hand, due to the low limitation of the amount of water samples passed at a time, it is not necessary to accumulate multiple experiments to complete the determination of DBPFP.

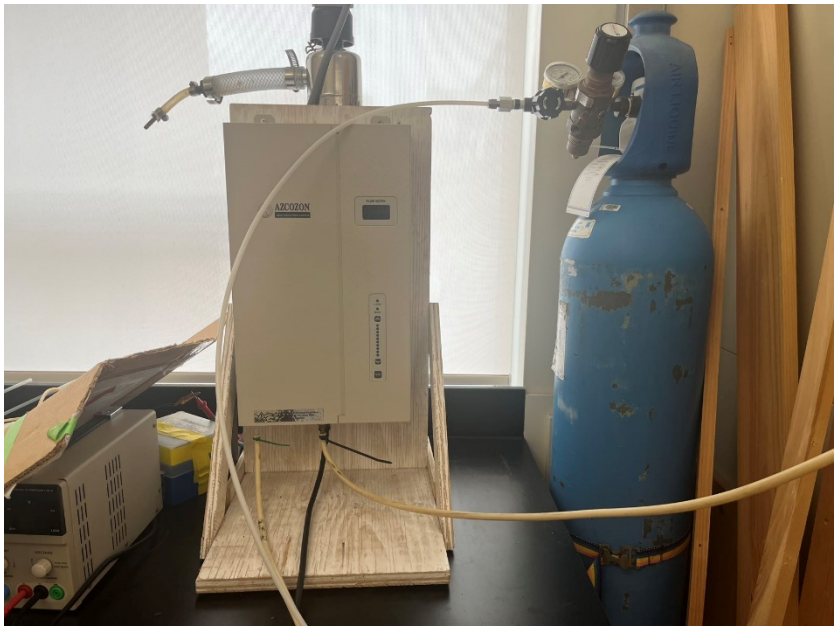

Figure 3-5 Ozone Generator

3.4 Hydroxyl Radicals Kinetics Experimental Design

A representative UV/H_2O_2 was chosen as a proxy in the experiments to determine UV advanced oxidizing radicals. Hydrogen peroxide is less susceptible to acid-base indicator reactions than chlorine, and hydrogen peroxide produces a single hydroxyl radical. In contrast, chlorine reacts with relatively complex radicals (Liu et al., 2020). Conversely, ozone will naturally degrade pCBA when it reacts with the pCBA in pure water and is unsuitable for this experiment (Park et al., 2004).

Milli-Q water was first used during the experiment to dilute the already configured pCBA stock solution at a concentration of 250 μmol/L and to configure the experimental reagents at 50 μmol/L. The reagents were used in the experiment as well. The pH of the reagent was measured to be around 4.3, and its effect was strongly related to the pH of Milli-Q water during the experiments. 1N NaOH and 1N HCl were used to adjust the pH to 5.5, 8.0, and 10.0 to study the effect of pH on the UV/H_2O_2 experiments, respectively. Similarly, in each experiment, the UV fluence was controlled to vary from 100, 500, and 1000 mJ/cm^2, and the concentration of hydrogen peroxide was adjusted from 1 mg/L to 10 mg/L.

0.5 ml of the sample was removed from each reaction, and another 10 μL of catalase was used to quench the residual hydrogen peroxide. Also, to ensure that the influencing factors of the experiment were determined, additional samples of hydrogen peroxide, hydrogen peroxide/catalase mixture, and UV irradiation were added to assess the stability of the

variables. All samples were placed in HPLC vials stored in a refrigerator at 4 degrees Celsius, and data were collected after the assay by the pCBA method in HPLC.

Chapter 4: Effects of AOPs on NOM and control DBP formation

4.1 Effects of UV-LEDs AOPs and Ozone on NOM

4.1.1 Exploring the Impact of AOPs on Basic NOM Parameters

This chapter completed the research on applying advanced oxidation to drinking water and comparing ozone to UV-LED AOPs. This chapter also compared the treatment effect before and after filters and comparing different media types. For its effect on NOM, the first step was to observe whether UV-LED treatment directly affected the value of DOC. For ozone advanced oxidation and UV-LEDs-related advanced oxidation the changes in DOC from each of the three different treatment (i.e., post sedimentation, post anthracite/sand filtration and post GAC/sand filtration) are plotted as shown in Figures 4-1 and 4-2. The changes in DOC for water are shown in Figure 4-1 using the concentration of ozone as the x-axis, and the names of the three different locations are labelled at the top of the figure. On Figure 4-2, UV-LEDs fluence is used as the x-axis, different colours represent the different doses of the oxides, and the type of the oxide class (H_2O_2/Cl_2) is marked above the locations.

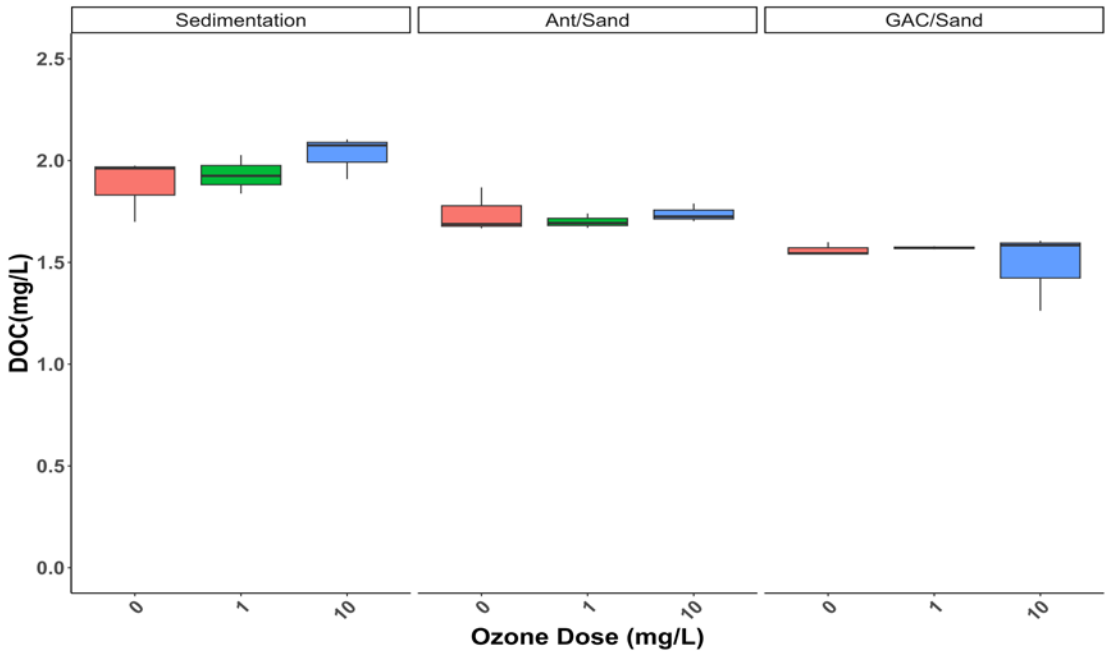

Figure 4-1 DOC Changes through Ozone AOPs

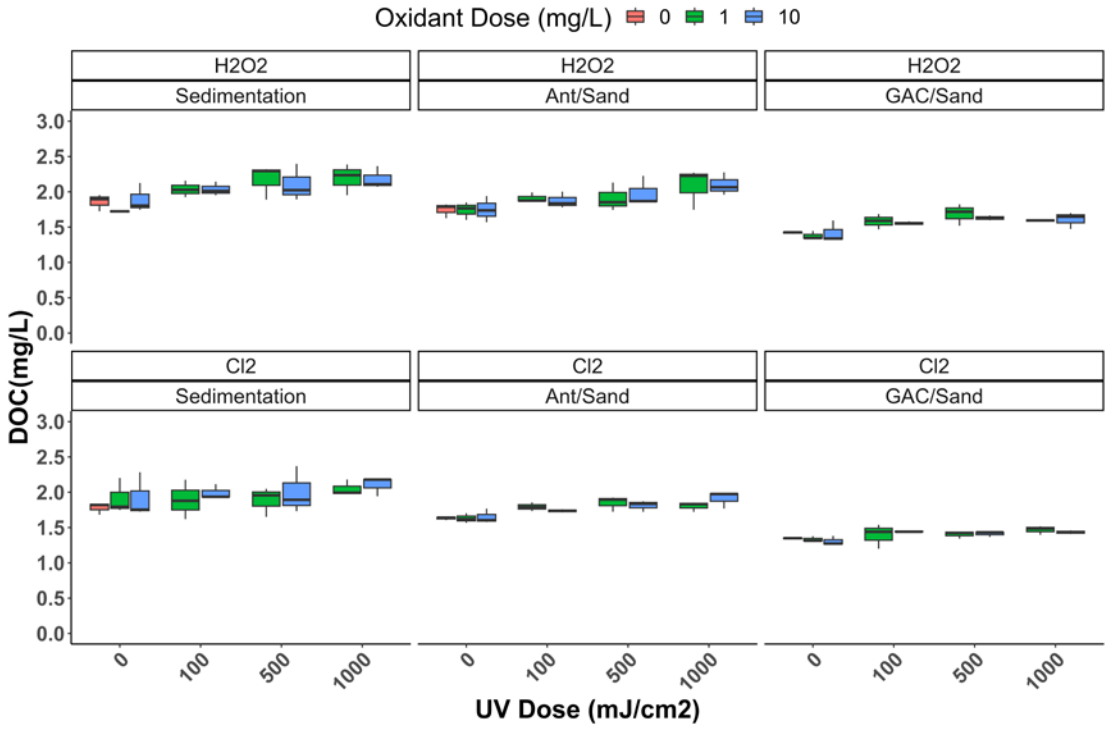

Figure 4-2 DOC Changes through UV-LEDs AOPs

In Figures 4-1 and 4-2, neither ozone advanced oxidation nor UV-related advanced oxidation has a significant effect on the DOC concentration of the different water sources. Therefore, advanced oxidation does not affect the DOC value of the water. This in agreement with previous studies on the direct reduction of DOC values by AOP is not applicable to this experiment, possibly due to the different water sources leading to different NOM or that the level of oxidation was not sufficient (Gil et al., 2019; Parsons, 2004).

In addition to DOC, as mentioned advanced oxidation may not completely degrade NOM directly, but it will convert large organic molecules into smaller ones (Tian et al., 2020; Toor & Mohseni, 2007). To prove this point, the SUVA value of UV_{254} was chosen as a parameter to be analyzed, and Figures 4-3 and 4-4, similar to the previous DOC, were made as shown below.

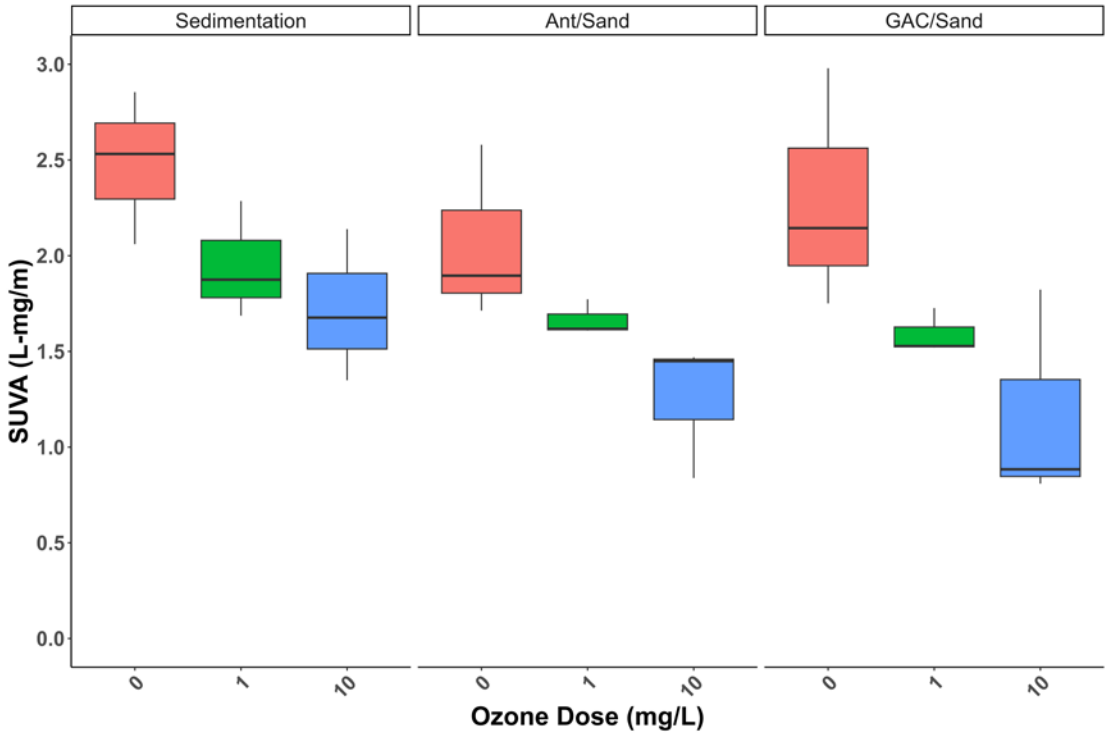

Figure 4-3 SUVA Changes through Ozone AOPs

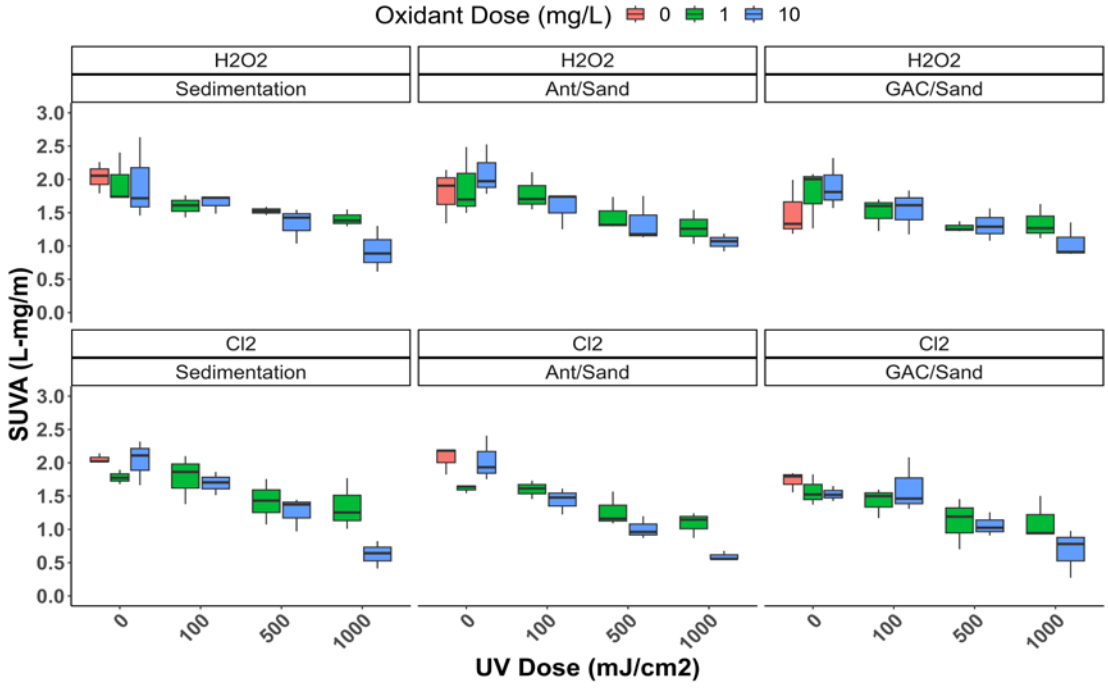

Figure 4-4 SUVA Changes through UV-LEDs AOPs

Both ozone and UV-related advanced oxidation directly reduced the SUVA value in the water. Combined with the invariance of DOC above, the main reduction in SUVA values can be can be linked to a reduction in UV_{254}. This indicates that all three types of advanced oxidation accomplished effective partial degradation of organic matter and that organic matter was not completely mineralized to CO_2 through oxidation. Regardless of the type of advanced oxidation used, it was found to result in very similar removal. (Anderson et al., 2023). For this reason, the Ant/Sand, the closest to the current water treatment process, will be selected as the object of analysis in the subsequent analysis.

4.1.2 Exploring the Effect of AOPs on NOM Compositions

In addition to further understanding the reason how the NOM changes in the water, the FRI volume in the water matrix is analyzed in the context of the FEEM with respect to each AOPs technique. The main FRI compositions were selected for analysis in this chapter are protein1, protein2, fluvic, microbial, and humic representing aromatic protein I, aromatic protein II, fulvic acid-like materials, soluble microbial materials, and humic acid-like materials.

According to this principle, the impact of traditional AOP ozone technology on FRI volume is plotted as shown in Figure 4-5 – Low Ozone denotes the result after treatment with an ozone concentration of 1mg/L and High Ozone is denotes the result after treatment with 10mg/L ozone. The water selected in this section is representative of Ant/Sand filtered water from the pilot plant.

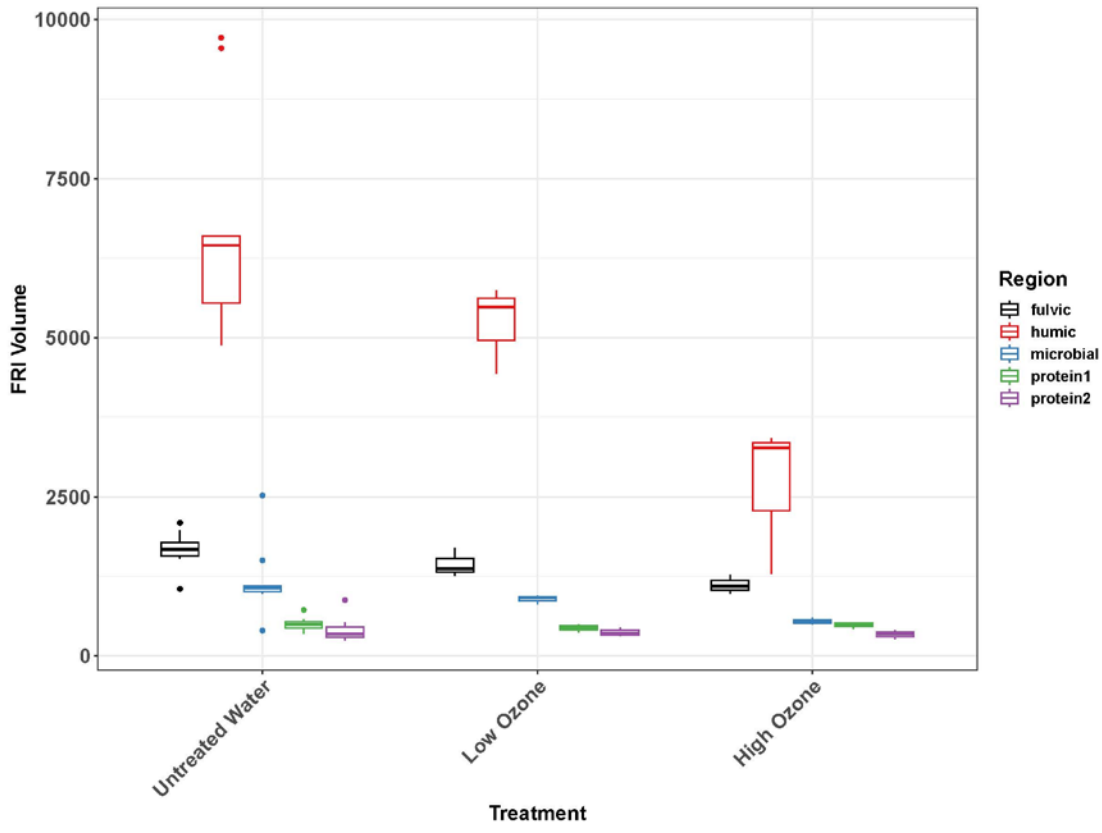

Figure 4-5 FRI Volume Changes through Ozone AOPs

According to Figure 4-5, humic acid-like materials in the untreated water have the highest volume in the selected fluorescence. The ozone AOP has very little effect on the removal of small organic molecules such as aromatic protein I, aromatic protein II, fluvic acid-like materials, and soluble microbial materials, but it had a good effect on the reduction of large organic molecules such as humic-like materials volume. It has been shown that ozone AOP technology has a stronger impact on the degradation of macromolecules (Gil et al., 2019; Parsons, 2004). A concentration of 1 mg/L ozone reduced the FRI volume of humus-like substances without advanced oxidation from about 7000 to about 5500, while 10mg/L ozone controls their FRI volume to about 4000. This may stem from the fact that humic-like materials have a lower oxidation potential and are more susceptible to oxidation and

decomposition by free radicals (Liu et al., 2020; S. MacIsaac, 2021; Matilainen & Sillanpää, 2010).

Similarly for UV-LEDs related AOPs the same method was used to make UV/H_2O_2 and UV/Cl_2 plots as Figure 4-6 and Figure 4-7 respectively, where Low/High oxidant (Peroxide or Chlorine) represents the oxidant concentration of 1mg/L/10mg/L, respectively. Low/Mid/High UV represents 100, 500, and 1000 mJ/cm^2 UV fluence, respectively. It is worth noting that during one of the hydrogen peroxide experiments, there was a special situation with the filters in the pilot plant during the water intake, which resulted in a high organic concentration, which in turn resulted in a large deviation in the data.

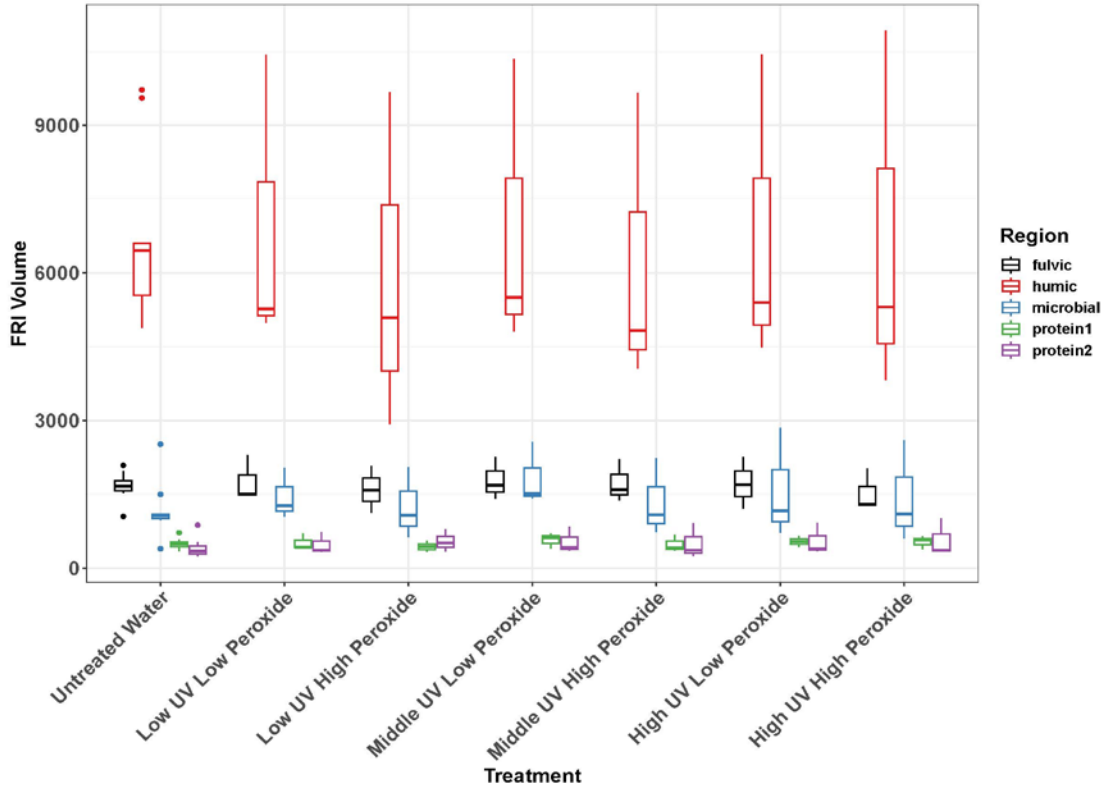

Figure 4-6 FRI Volume Changes through UV/H_2O_2 AOPs

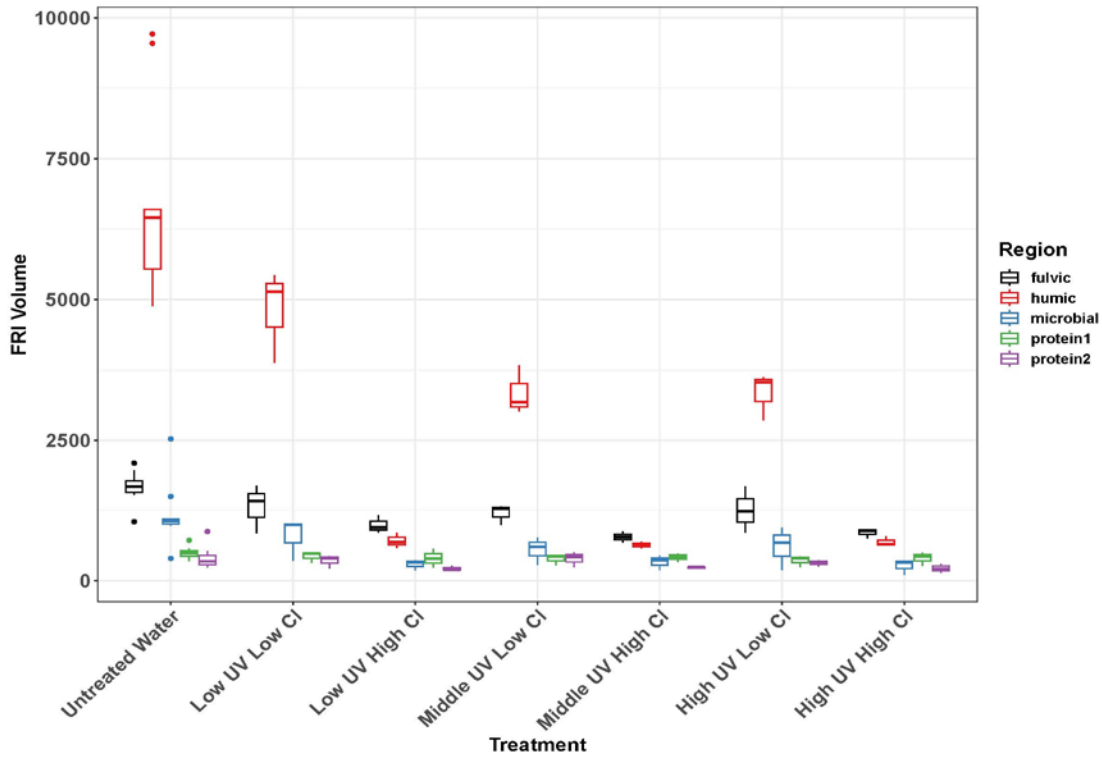

Figure 4-7 FRI Volume Changes through UV/Cl_2 AOPs

In general, the effects of UV-LEDs AOP and conventional ozone advanced oxidation on FRI volume are generally consistent, and the main effects are still reflected in humic-liked materials. In a sequential view, the effect of UV/H_2O_2 on FRI volume is less pronounced compared to UV/Cl_2, but the median value of humic-liked materials still decreases with the concentration of hydrogen peroxide as well as with the increase of UV fluence, and the result is very similar to the decrease of SUVA value. UV-LEDs/H_2O_2 in the presence of 1000 mJ/cm^2 UV fluence as well as 10 mg/L of hydrogen peroxide successfully reduced the FRI volume of humus-like material from untreated 7000 to about 5300.

As for UV/Cl_2 advanced oxidation, it was first found that the amount of humic could be found to decrease with increasing UV fluence at the same oxidant dose. For example, at a chlorine concentration of 1 mg/L, the FRI of humic species at 100 mJ/cm^2 decreased from an initial value of about 7,000 to a value of about 3,000 at 500 mJ/cm^2. It is noteworthy that it seems that high concentrations of chlorine have a great influence on the humic experiments, as long as 10 mg/L concentration of chlorine was involved in the reaction, the amount of humic appeared to be greatly decreased. It may be that the decrease in humic is caused by the reaction of humic with chlorine in water rather than all by free radical reactions. This may also be one of the reasons why the SUVA value in the previous section was reduced to 0.6 in the case of AOPs with high chlorine concentration.

4.1.3 Exploration of Mechanisms of UV-LEDs AOPs

Since UV-LEDs AOPs are different from ozone, the reaction consists of both UV and oxides, and the main body of the reaction of AOPs is again free radicals. Therefore, to investigate the role of advanced oxidation reaction of UV-LEDs, UV-LED/H_2O_2 is selected as a representative in this section, and the detection of free radicals is used to discuss what causes the change of NOM in the previous section, and its influencing factors.

To accurately probe the production of hydroxyl radicals (OH •) in the advanced oxidation reaction of UV-LEDs as a light source, and to consider both the effect of oxide concentration, and the effect of pH on the reaction. The concentration of pCBA was measured at 0-1000mJ/cm^2 under three different pH conditions with different

concentrations of hydrogen peroxide of 0, 1 and 10mg/L. The linear prediction graphs with ln(pCBA) as the y-axis and UV fluence as the x-axis are shown in Figure 4-8 below.

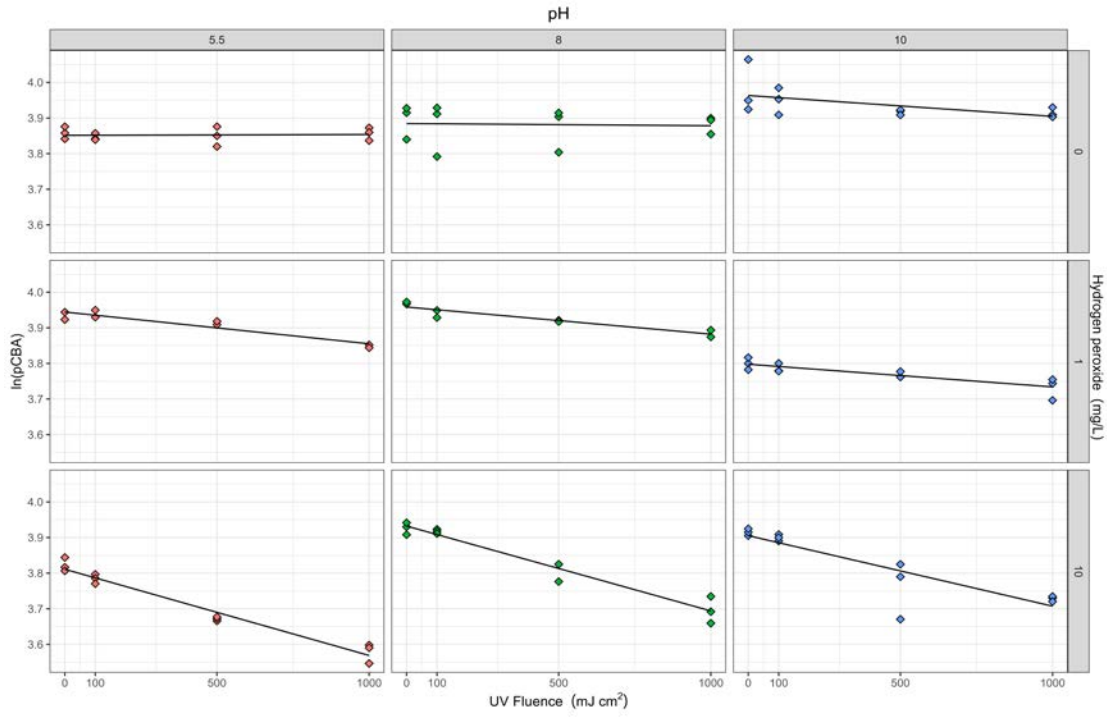

Figure 4-8 The slope of the linearity in the reaction kinetics studies of UV and UV/H_2O_2 based AOP represents the luminous flux corresponding to the first-order reaction constants for generating OH · radicals.

From the trend line graph, it can be observed that there is almost no degradation ability of pCBA at pH 5.5, 8 when utilizing only UV-LED without hydrogen peroxide. Moreover, it can be found that the only degradation trend at pH 10 is due to a large shift in the initial concentration of one group of samples, whose ln(pCBA) value exceeds 4, which may be attributed to an error in the experimental operation. Overall, the use of UV-LEDs alone did not result in the degradation of pCBA. However, the degradation of pCBA was

accomplished to a certain extent at either 1 or 10 mg/L H_2O_2. One possible reason that using a 280 nm LED with pCBA to generate free radical generation may not be ideal is that there is a small overlap between the absorption of pCBA and the 280 nm output of the LEDs.

In the case of UV-LEDs coupled with hydrogen peroxide, a similar linear decrease in pCBA values was observed at both 1 mg/L and 10 mg/L, with characteristics consistent with previous UV-LEDs AOP studies and indicative of free radical production(S. MacIsaac, 2021; Rosenfeldt et al., 2005, 2006). Further, it can be found that comparing its slope, i.e., the k value, it is intuitively obvious that the k value of the 10 mg/L group is larger than that of the 1 mg/L group, and the results are also in line with previous studies and reflect that the concentration of H_2O_2 plays a positive correlation role in the UV-LEDs AOPs (S. MacIsaac, 2021).

To better represent the data, after the data processing of the above table will be plotted as Figure 4-9. In addition to the previously mentioned deviation at pH 10, the yield of free radicals produced at 0 mg/L H_2O_2 is relatively small, which is a significant deviation from the results produced by conventional UV mercury lamps (Rosenfeldt et al., 2006). In the UV/H_2O_2 reaction, the lower the pH under the same H_2O_2 concentration, the higher the yield of free radicals. The pH pattern is generally consistent with previous research on UV mercury lamps (S. MacIsaac, 2021). Also, the production of free radicals increases with the amount of hydrogen peroxide at the same pH. In addition, the rate of free radical production increases with increasing hydrogen peroxide at the same pH, with the yield of

10 mg/L H_2O_2 being more than three times that of 1 mg/L. The rate of free radical production is also higher at pH 5.5 and 8, with the yield of 1 mg/L H_2O_2 being more than three times that of 1 mg/L. In contrast, compared to the UV-only reaction, the yield of 1 mg/L H_2O_2 is more than 10 times higher at pH 5.5 as well as 8. Furthermore, the comparison found that under the same conditions, the UV-LED-directed H2O2 reaction produces only about 20% of the free radicals of mercury lamps(S. MacIsaac, 2021; Rosenfeldt et al., 2006).

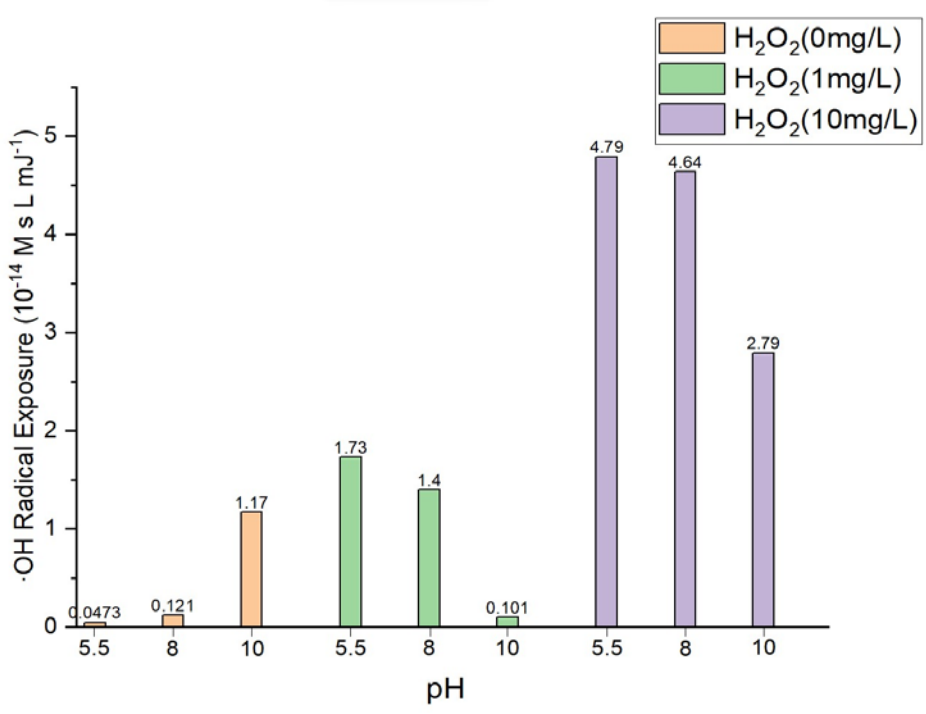

Figure 4-9 Different *ROH* produced by different AOPs

The experiments in this section demonstrate through the values of free radicals that UV-LEDs AOPs are oxides reacting with UV to degrade NOM. And it is proved that the value of radicals increases with the increase of UV fluence and oxide dose, which is

consistent with the trend of SUVA in the previous section. This is a good indication that the oxidizing ability of UV-LEDs AOPs is correlated with the number of free radicals produced, while UV fluence, oxidant dose, and pH are all influencing factors.

4.2 Comparison of UV-LEDs AOPs and Ozone on Drinking Water

4.2.1 Comparison of AOPs on SUVA

Since the experimental results for the three water bodies showed similar results in the prequel results, Ant/Sand filtered water from the pilot plant was selected for this section and for subsequent experiments. To compare the three AOPs technologies more intuitively, the highest dose in the ozone advanced oxidation process, i.e., 10 mg/L of ozone-treated water, was chosen in this chapter to compare with the highest dose in the two UV-related advanced oxidations, i.e., 10 mg/L of H_2O_2 or Cl_2 in combination with 1000 mJ/cm^2, as a representative. For its processing effect, the SUVA value is a parameter for graphing, as shown in Figure 4-10.

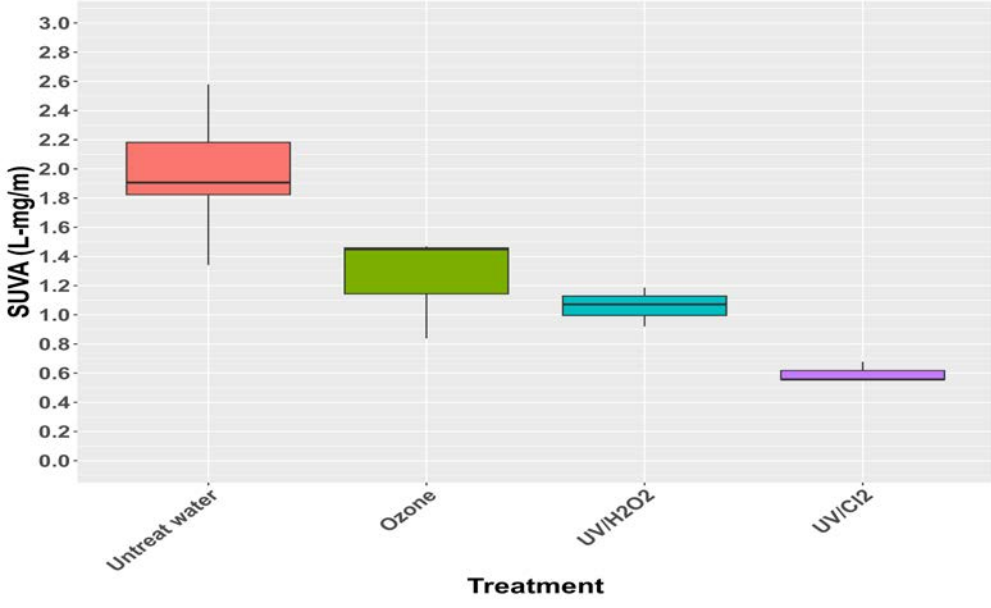

Figure 4-10 SUVA Comparison for Different AOPs

As shown in Figure 4.10, the SUVA value of the original un-advanced oxidized water sample was around 1.9 L • mg/m, and was reduced to around 1.4 L • mg/m after ozone treatment. For UV-LEDs-related advanced oxidation, it is evident that the reduction of SUVA value is better. UV-LEDs/H_2O_2 reduced the SUVA value to about 1.1 L • mg/m, and UV-LEDs/Cl_2 reduced the value to about 0.6 L • mg/m. The analysis reveals that UV-LEDs advanced oxidation results better than ozone alone in reducing SUVA values, with UV-LEDs/Cl_2 being the best of the technologies. This echoes the results of many previous studies (Farzanehsa et al., n.d.; Lamsal et al., 2011; Miralles-Cuevas et al., 2017; Rosenfeldt et al., 2006).

4.2.2 Comparison of AOPs through NOM Composition Changes

To compare the effects of the different techniques on the water matrix, the results at the highest oxidation conditions (10mg/L ozone, 1000mJ/cm^2 UV + 10mg/L Chlorine/Peroxide) of the three AOP techniques were collated. Combining this with the data from the untreated water matrix is shown in Figure 6-4. The mapping is done in the same way as in the previous section for the separate AOP technique. Untreated water in this section, including those that follow, refers to waterbodies taken out of Ant/Sand that have not been treated by AOPs.

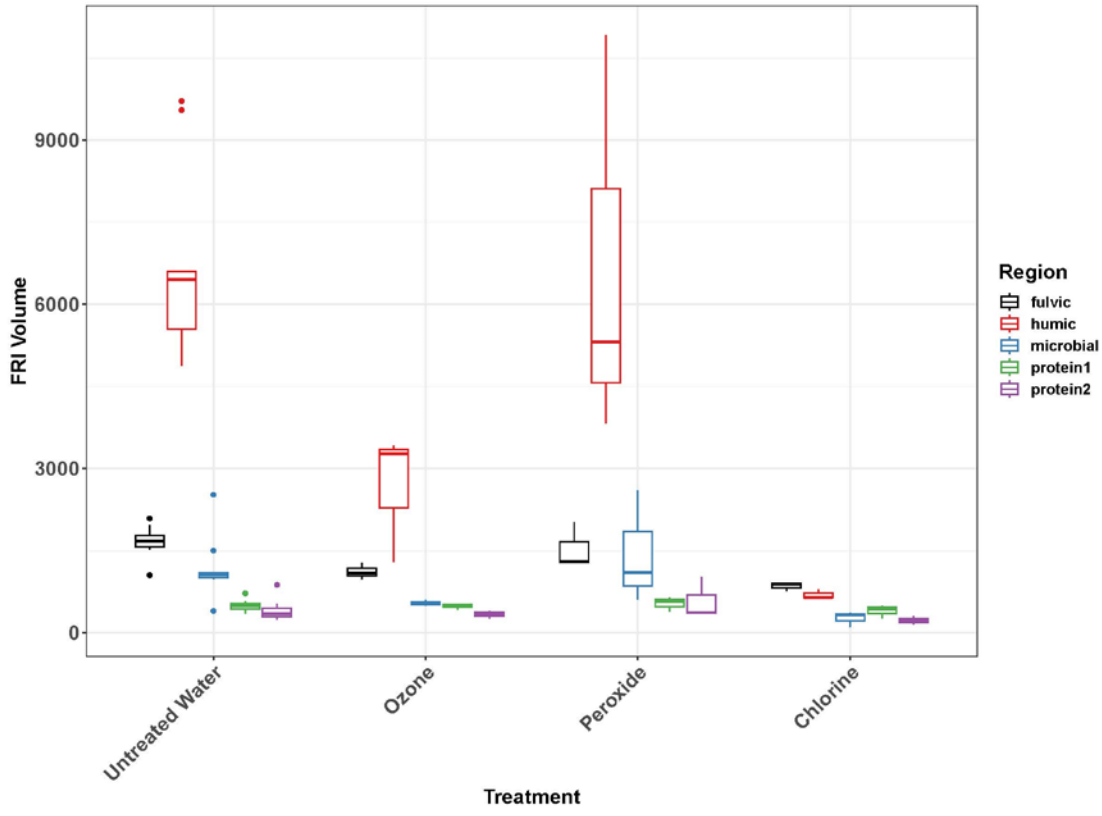

Figure 4-11 FRI Volume Changes for Different Treatment

From this figure, it can be seen more clearly that at high doses of AOP, fulvic acid-like materials, soluble microbial materials, and humic acid-like materials can be removed from the water, while there is little removal of the two proteins. This also confirms the potential of UV AOPs to remove micropollutants as well as fluvic if it is at high intensity in previous studies (S. MacIsaac, 2021). The main part that can be removed by AOP is the humic-liked materials, and then it is found that UV/H_2O_2 has a lower removal rate for humic-liked materials compared to UV/Cl_2 and Ozone. UV/Cl_2 can be found to have the best humic removal compared to ozone and UV/H_2O_2. When the FRI volume of humic-like substances in untreated water reached a concentration of approximately 7000, optimal

control efficacy was observed. This was achieved through the application of a UV fluence of 1000mJ/cm^2, accompanied by the introduction of UV-LEDs and Cl2 at a concentration of 10mg/L. This treatment regimen resulted in a significant reduction of the FRI volume to approximately 800 units. Concurrently, employing UV-LEDs in conjunction with H_2O_2 and ozone at the same concentration of 10mg/L under similar conditions yielded varying outcomes. Specifically, the FRI volume decreased to 5300 units with UV-LEDs/H_2O_2 treatment, and to 4000 units with ozone treatment.

4.2.3 Comparison of AOPs through DBPFP

Although advanced oxidation has been successful in reducing SUVA in water, it does not directly follow that the potential for DBPs in treated water has necessarily been reduced. Therefore, in this section, UFC experiments were performed on the water samples before and after treatment to explore the production of THMFP. The values of THMFP treated by different treatment processes are shown in Figure 4-12.

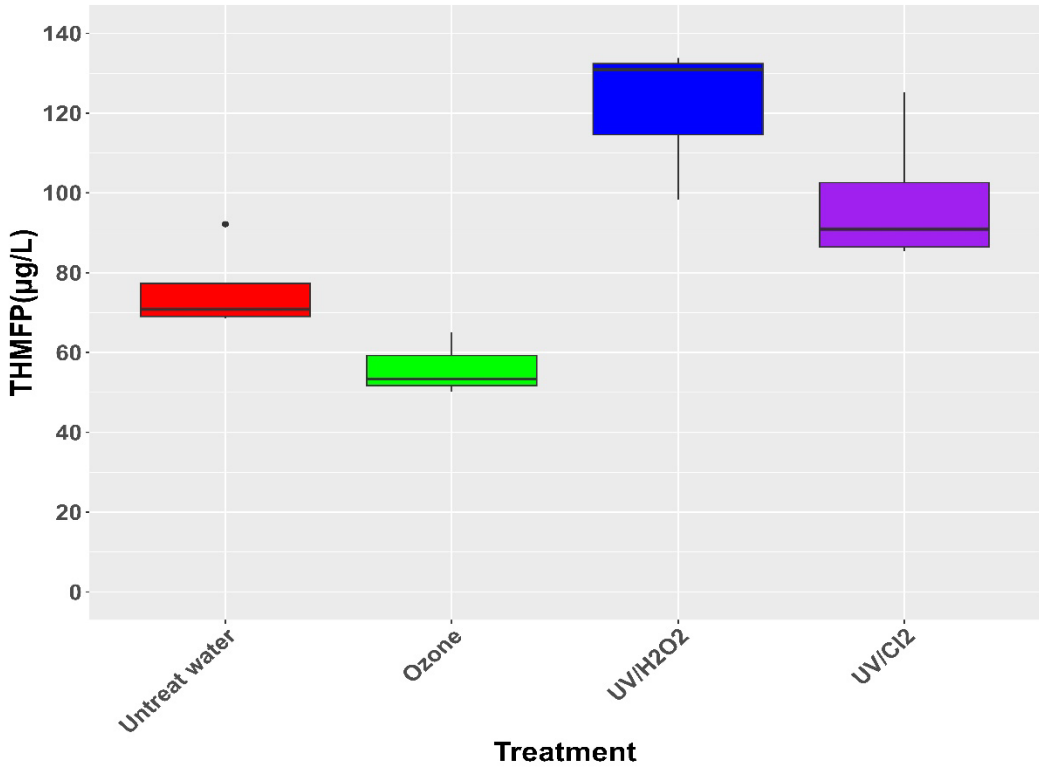

Figure 4-12 THMFP for Different Treatment

From the figure, it can be noticed that after the ozone advanced oxidation reaction, THMFP showed a similar decrease compared to the untreated water samples as the decrease in SUVA values, making it decrease from around 70µg/L to around 50µg/L. Unexpectedly, however, in complete contrast to the SUVA values, UV/H_2O_2 and UV/Cl_2 elevated THMFP to about 130µg/L and 90µg/L, respectively. This proves that SUVA is not applicable to predict the production of THMs after UV advanced oxidation. This result is very similar to previous results using UV MP AOPs to treat organic matter in water. Many of these studies found that at 1000 mJ/cm^2, even though there was a decrease in the SUVA

value of the water body, its DBPFP value did not decrease with the decrease in SUVA (S. MacIsaac, 2021; Matilainen & Sillanpää, 2010; Toor & Mohseni, 2007).

4.2.4 Comparison of the Practical Use of UV-LEDs and Ozone

However, it is incomplete to evaluate the potential of UV-LEDs equipment versus ozone in the field of water treatment only in terms of treatment effectiveness. The goal of this study is to establish a more resilient treatment system in the face of high NOM drinking water bodies that will be more difficult to treat in the future, and therefore the cost, ease of installation, and subsequent impact on the environment are all considered in the consideration of AOPs technology (Gil et al., 2019; Andreozzi et al., 1999). Therefore, the comparison between UV-LEDs and ozone in the field of water treatment will be discussed next from the application point of view.

In terms of installation and use, even though ozone is a relatively mature water treatment technology, most of the time the entire water treatment system is still redesigned and constructed, due to its footprint and the need for liquefied oxygen as a gas reserve, making it relatively large space requirements (Rice, 1996; Suty et al., 2004; Tichonovas et al., 2017). However, although UV-LEDs have not been put into production since they were designed, the flexible design nature of the LEDs makes it possible to complete the design by retrofitting them to existing equipment (Beck et al., 2017; Jarvis et al., 2019; Song et al., 2016). Moreover, except for the LEDs, there are no other specific facilities or space required for the equipment to be completed (W. Yang et al., 2014). Previous experiments

have shown that it can be installed in different areas before and after filtration and different treatment methods combined to ensure the flexibility of its design.

In the direction of energy saving and cost, the main energy consumption of both ozone and LEDs equipment is in electricity, but ozone treatment requires not only a larger equipment space as mentioned in the previous paragraph, but also the cost of oxygen reserve (Marda et al., 2008; Rice, 1996). Compared with UV MP equipment, because UV-LEDs do not need to warm up time, will not reduce the luminous power with the passage of time, and less heat and the direction of the reverse in the direction of light, more energy efficient (Beck et al., 2017; Hölz et al., 2017; Jarvis et al., 2019; S. A. MacIsaac et al., 2023; Song et al., 2016).

From the level of environmental protection, LEDs lamps have a long life, no mercury pollution, LEDs light has been studied at specific wavelengths on biological impact is small, such as 222nm UV-LEDs (Jarvis et al., 2019; Schaefer et al., 2007; Yamano et al., 2020). Ozone equipment can not be avoided gas emissions and production is undoubtedly for the environment (Matilainen & Sillanpää, 2010; Rice, 1996). Overall, even though UV-LEDs are relatively immature compared to ozone technology, they have greater potential.

4.3 Analysis and Summary

4.3.1 UV-LEDs AOPs and Ozone on NOM and DBPFP Control

First, this chapter analyzes the effect of elemental advanced oxidation on NOM in water through basic parameters such as DOC, SUVA and FRI volume. The first and most direct finding is that the three different advanced oxidation techniques do not significantly reduce DOC, which may be due to two reasons. The first is that the advanced oxidation techniques do not directly reduce DOC but can only degrade organic matter macromolecules into small molecules; the second is that the oxidant dosage as well as the UV fluence of the advanced oxidation techniques in this chapter do not reach the value for DOC degradation. Because none of the UV fluence in this experiment exceeded 1000 mJ/cm^2, it was found in a previous study that this level of UV could not fully mineralize NOM (Matilainen & Sillanpää, 2010; Toor & Mohseni, 2007).

Therefore, for SUVA values, all three advanced oxidations accomplished significant reductions. This demonstrates that advanced oxidation completes the reaction to NOM in water and significantly reduces the absorbance of organic matter in water, especially UV_{254}. This further proves the reaction mechanism that AOPs mainly degrade large organic molecules into small ones under the conditions of this experiment (Matilainen & Sillanpää, 2010). Moreover, it can be found that the advanced oxidation technology has similar treatment results for different water locations, i.e., it has a very good universality. It can be applied to all aspects of water treatment.

A comparison of representative experimental groups showed that the UV-related advanced oxidation technology was more effective in reducing SUVA than ozone advanced oxidation. This also demonstrates that UV-LED related AOP has the potential to replace traditional advanced oxidation technologies such as ozone advanced oxidation. Furthermore, the UV-LEDs related AOP technology is close to or even better than the conventional ozone process in terms of SUVA reduction for drinking water. For UV-LED-related AOPs, the UV/Cl_2 technology clearly demonstrated better results, almost reducing the SUVA value to about 0.6 at high doses of oxidizer with high doses of UV fluence.

Summarily results occurred for FRI volume changes after three AOPs. After three AOP treatments, both ozone, UV/H_2O_2, and UV/Cl_2 showed a reduction in FRI volume, especially for humic-liked materials. And such reductions are enhanced as the strength of the AOP increases. It is noteworthy that advanced oxidizing conditions with high concentrations of chlorine reduced humic-liked materials in water to very low values regardless of the intensity of UV. It is possible that the high concentration of chlorine reacts with humic extremely easily and this may also be the reason why DBPs are generated.

By comparing the results of the three high-intensity AOP, it was found that UV advanced oxidation at high intensity had a good effect on micro-pollutants and fluvic-type organics but had a poor effect on proteins. The treatment effect for humic is UV/Cl_2 > Ozone > UV/H_2O_2. However, the effect of chlorine is not necessarily all from the advanced oxidation as shown in the previous section. Such processed data is still a very preliminary

representation of the effect of AOP on the water matrix but is not comprehensive enough, more data and experiments need to be completed.

Moreover, in the comparison of UV-related AOP experiments, it was found that UV/Cl_2 had a better treatment effect compared to UV/H_2O_2, in order to analyze the reason for this, the spectrograms of the UV-LED used in this chapter from 190 nm to 400 nm were extracted and plotted together with the absorbance of 10 mg/L H_2O_2/Cl_2 in the same wavelength interval as shown in Figures 4-13

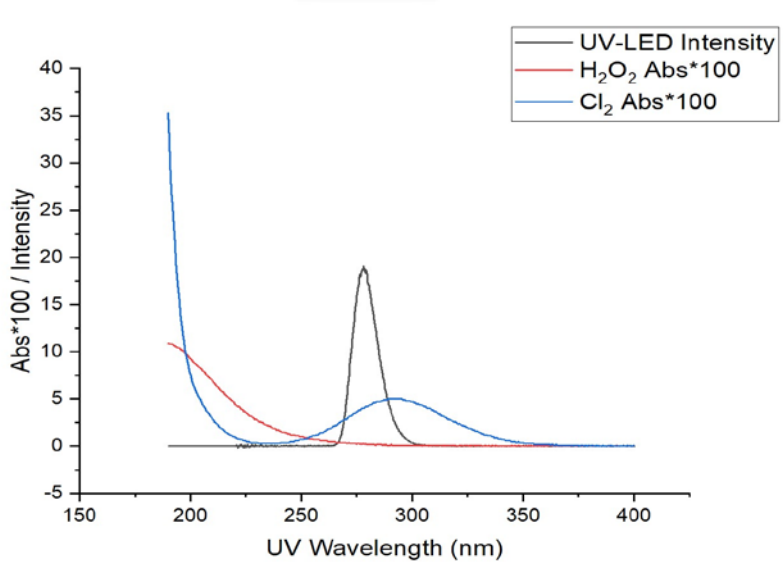

Figure 4-13 Spectrum for UV-LED combined the absorbance of Cl_2 and H_2O_2

It can be noticed that the peak wavelength of absorbance of the H_2O_2 solution should be below 190 nm, while it has almost no absorbance at the peak wavelength of 280 nm of the UV-LED. On the contrary, although the peak value of the Cl_2 solution should also be lower than 190nm, it has an obvious lower peak absorbance at about 280nm. Such a discrepancy may explain why the SUVA reduction of UV/Cl_2 is significantly better than that of

UV/H_2O_2. This also demonstrates that wavelength dependence influences UV-related advanced oxidation and deserves to be investigated in the future.

While both SUVA and FRI volume represented the amount of organic matter in the water as well as its composition in a reasonable manner; however, their comparability to DBPFP was not reliable. Compared to the original water samples, the ozonated water produced a similar decrease in THMFP as the SUVA values. Surprisingly, after the UV-LEDs AOP reaction, the THMFP values did not decrease, but rather increased. In particular, UV/H_2O_2 even exceeded 100μg/L, which showed similar results to previous studies using UV MP advanced oxidation (S. MacIsaac, 2021; Matilainen & Sillanpää, 2010; Toor & Mohseni, 2007). Below 1000 mJ/cm2 , when the values of oxides were not high, THMFP in all these studies showed an increasing trend(S. MacIsaac, 2021; Toor & Mohseni, 2007). The rise in THMFP due to UV/Cl_2 may be due to excess chlorine and the ratio of chlorine to UV fluence.

4.3.2 Mechanism of UV-LEDs AOPs and Differences from UV MP

The results indicate that of the hydroxyl radicals in the advanced oxidation reaction occurring in the experiment with UV-LEDs/H_2O_2 come from the combined action of UV and H_2O_2, and the degradation of pCBA cannot be accomplished using 280nm UV-LEDs alone. This is a different conclusion from the previous results using UV medium pressure mercury lamp (UV MP), to explore the reason, respectively, 280nm UV-LED and UV MP spectral detection spectra in the interval of 200nm to 400nm, combined with the same wavelength interval for the absorbance of 50μmol/L pCBA to complete the plotting. To

visualize the pictures, the absorbance was multiplied by 10 orders of magnitude to make the pictures more contrasting.

As shown in Figure 4-14, UV MP has a more comprehensive spectral wavelength range, while UV-LED is more concentrated in the 280 nm range. It happens that the main absorbance interval of pCBA is concentrated around 230 nm, where UV MP retains some intensity, while on the contrary UV-LEDs have almost no intensity in this radiation band, which could explain the difference in the results. It can also be conjectured that 230 nm wavelength UV light alone should be optimal for the degradation of pCBA. In recent years, the application of 222 nm UV Kr-Cl lamps in the field of disinfection has had a very good progress, and this experiment suggests the use of 222 nm UV instrumentation for pCBA to conduct experimental studies to verify the conjecture of this experiment (Rosenfeldt et al., 2005; Yamano et al., 2020).

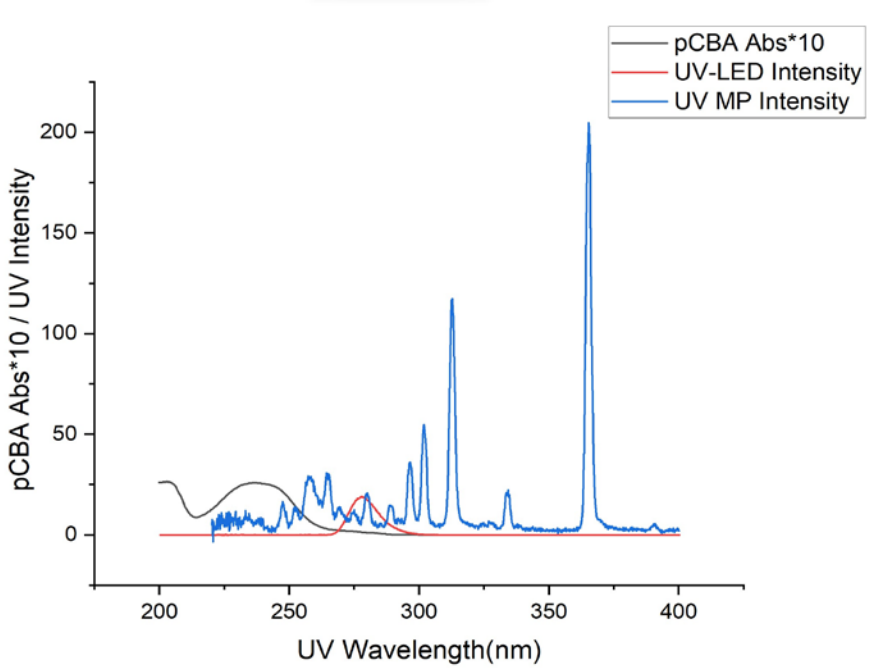

Figure 4-14 Spectrum of UV-LED / UV MP combined absorbance of 50µmol/L pCBA

The experiments prove that advanced oxidation by UV-LEDs is mainly drive by radicals. This work also demonstrates some of the differences as to why the oxidative effect of conventional UV MP is different for UV-LEDs. This difference is reflected in the difference of the method of calculating the dose of UV fluence used in the study mentioned before (S. MacIsaac, 2021). The method used in this paper utilizes a UV sensor in combination with several factors to calculate UV fluence, considering the UV-T of a solution at a specific wavelength, whereas the method used in the previous paper is not as well developed and does not utilize the same sensor, and more experiments would need to be completed before accurate conclusions could be drawn.

Overall, the most representative UV/ H_2O_2 was selected in this chapter for UV-LEDs AOP mechanism studies through the pCBA approach. Firstly, it was found that the degradation of pCBA could hardly be accomplished using only 280 nm UV-LEDs, which may be since the absorption bands of 280 nm UV and pCBA do not overlap. At the same pH and UV fluence, 10 mg/L H_2O_2 produced more radicals than 1 mg/L H_2O_2, which indicated that the concentration of H_2O_2 had a positive effect on the reaction. Meanwhile, this experiment found that lower pH under the same condition can produce more free radicals, which may be related to the morphology of hydrogen peroxide in water. This gives a good suggestion for the practical use of UV-LEDs AOPs, which have better results at relatively low pH if high doses of H_2O_2 are used as an oxide.

Chapter 5: Conclusions and Recommendations

5.1 Conclusions

The objectives of this thesis were to 1) explore the effects of novel UV-LEDs AOPs as well as conventional ozone reactions on NOM in drinking water, 2) investigation of changes in the composition of water after AOPs and its association with DBPFP, and 3) compare three advanced oxidation technologies, including ozone, UV-LEDs/H_2O_2 and UV-LEDs/Cl_2, for the treatment of water from three different locations in the drinking water treatment process. The specific conclusions for each of the three objectives are summarized below.

5.1.1 Effect of AOPs on NOM in Pilot Treated Water

With regards to the impact on NOM, this work demonstrated that neither of the UV-LED AOPs (e.g., UV-LED/Cl_2 or UV-LED/H_2O_2) nor the ozone caused direct changes in the concentration of DOC under the treatment conditions explored in this study (e.g. 1000mJ/cm^2 and 10 mg/L oxidant). The reason for this is that the oxidation at 1000 mJ/c m^2 and 10 mg/L oxidant, as well as ozonation at a dose of 10 mg/L did not completely mineralize NOM. Instead, these treatments partially-transformed or degraded NOM, resulting the conversion of NOM macromolecules into smaller molecules, similar to that observed in previous studies (S. MacIsaac, 2021; Matilainen & Sillanpää, 2010; Sgroi et al., 2021; Toor & Mohseni, 2007). A higher oxidant dosage and UV fluence would be required for complete oxidation/mineralization, but this would also increase the operating cost of the process for practical use.

In addition, the change in the SUVA supportive of the trend of NOM degradation through ozone and UV-LEDs AOPs. For the ozone reaction, the SUVA values show a gradual decrease from the original (e.g., pilot treated) values as the ozone concentration increases. This is in agreement with previous similar experiments (S. MacIsaac, 2021). The SUVA value of Ant/Sand water source in the 10 mg/L ozone reaction condition decreased from 1.9 L • mg/m to about 1.5 L • mg/m. A similar trend was observed for the UV-LEDs AOPs related reactions, where the degree of decrease was related to both UV fluence and the dose of oxidant (e.g., Cl_2 or H_2O_2). As the oxidant dose increases with UV fluence, the value of the change in SUVA increases.

The reason for the superior performance of UV-LEDs/Cl_2 compared to UV-LEDs/H_2O_2 in this study may be that chlorine has a much higher absorption around 280 nm UV light compared to hydrogen peroxide. Therefore, under the same conditions, chlorine absorbs the UV light emitted by 280 nm UV-LEDs more readily to produce free radicals to oxidize NOM, which demonstrates the close relationship between the absorbance of the oxide and the selected UV wavelength. Also shown is another important factor that determines the effectiveness of UV-related AOPs, the effect of the wavelength of the UV. As for this experiment, the results of the experiment are biased for chlorine due to the 280 nm UV-LEDs used in the experiment. It cannot be said that the conclusion is applicable for all wavelengths of UV-LEDs. Another reason why chlorine-related reactions work better compared to hydrogen peroxide reactions is that the reaction is aided by not only hydroxyl

radicals but also chlorine-related radicals (Liu et al., 2020; Sun et al., 2016). This may have led to the difference in the effectiveness of the reaction.

The relationship between UV fluence, oxidant and advanced oxidation efficacy was also explored in this research by measuring the pCBA concentration before and after treatment. The use of pCBA also allowed the exploration of mechanisms and influencing factors of the UV-LED/H_2O_2 AOPs reactions. The mechanism of 280nm UV-LEDs AOPs primarily involves the generation of hydroxyl radicals through the synergistic effect of UV light and oxidants, a process not achievable by 280nm UV-LEDs or oxidants alone. This sheds light on the unique pathways of degradation enabled by UV-LEDs AOPs compared to conventional methods like ozone. The generation of free radicals increases with the co-increase of UV fluence and oxidant, which explains why the decrease in SUVA values appears to be positively related to the dose of both.

5.1.2 Impacts of NOM Composition and DBPFP after AOPs

Using florescence measurements, it was identified that the main NOM constituents in the experimental waters were humic-like in nature. Furthermore, all three AOPs treatments—ozone, UV/H_2O_2, and UV/Cl_2 showed some reduction in FRI volume, especially for humic-like substances. When the FRI volume of humic-like substances in untreated water was about 7000, highest intensity UV-LEDs/Cl_2 AOPs (UV fluence of 1000mJ/cm^2 and chlorine of 10mg/L) achieved the best control effect and reduced the FRI volume to about 800. At the same time, UV-LEDs/H_2O_2 under the same conditions (1000mJ/cm^2 UV + 10mg/L H_2O_2) and 10mg/L ozone reduced the FRI volume to 5300 and 4000, respectively.

This reduction was enhanced with increasing AOPs intensity, which was paralleled by the reduction trend of SUVA. This may be related to the greater absorbance of humic substances at around 254 nm. It is noteworthy that advanced oxidizing conditions with high chlorine concentrations can reduce humic-like substances in water to very low values independent of UV intensity. Further, the three AOPs were found to be effective for the degradation of micropollutants and humic substances, but less effective for proteins. For humic substances the treatment effect was in the order of UV-LEDs/Cl_2 > ozone > UV-LEDs/H_2O_2. In the UVLED/Cl_2 advanced oxidation, increasing fluence with constant oxidant doses led to decreased in humic concentration. For instance, when the chlorine concentration was 1 mg/L, the FRI of humic species at 100 mJ/cm² decreases from an initial value of approximately 7,000 to around 3,000 at 500 mJ/cm². Notably, even low UV as low as 100 mJ/cm^2 with 10mg/L chlorine significantly reduced humic content, suggesting a reaction between chlorine and humic compounds in water.

Through advanced oxidation reaction with ozone, the reduction trends in THMFP values were similar to the reduction in SUVA values as well as humic FRI values, corresponding to concentrations from about 70 µg/L to about 50 µg/L when compared to water samples treated with no ozone. In contrast to it, the THMFP values of the water samples treated with the highest intensity UV-LEDs AOPs in this study showed an increasing trend in THMFP. The UV-LEDs/H_2O_2 and UV/Cl_2 treatments resulted in THMFP levels of approximately 130µg/L and 90µg/L, respectively. This indicates that FRI values and SUVA values were not reliable predictors of THMFP production post UV-LEDs advanced oxidation. Similar findings were observed in previous studies utilizing medium pressure

mercury based UV AOPs (S. MacIsaac, 2021; Toor & Mohseni, 2007). In conjunction with previous studies, the hypothesis of this study is that for UV fluence under 1000 mJ/cm^2, both UV-LEDs AOPs and ozone AOPs produce low molecular weight compounds, that vary in size, with ozone AOPs forming the smallest compounds. This difference in oxidation byproducts suggests that the portion of NOM that initially reacts with ozone in the aqueous matrix is more oxidized compared to UV-LEDs AOPs. The partial oxidation of NOM provides additional reactive material for DBP formation, although additional data are needed to confirm these relationships (S. MacIsaac, 2021; Matilainen & Sillanpää, 2010; Tian et al., 2020).

Not only that, for the ozone experiments, the test experiments for DBPFP were done once in a flow-through system, while the advanced oxidation associated with UV-LEDs was experimented in a 130 ml petri dish, which required multiple reaction experiments to be completed due to the amount of water samples. The intervals between their experiments could not be avoided, and excess oxides may influence DBPFP. This will make the comparison of the experimental results somewhat biased. It cannot fully represent the performance of the two technologies in practical applications.

5.1.3 Comparison of Three Advanced Oxidation Technologies.

This study showed that the effect of AOPs treatment was comparable in terms of SUVA and DOC for samples collected both before and after filtration. This demonstrates the flexibility of AOPs in drinking water treatment systems and specifically in terms of the location of UV AOPs in the treatment train.

This work also showed UV-LEDs AOPs demonstrated a greater treatment capability compared to ozone for the removal of SUVA with humic substances and other NOM components. In a comparison of the highest doses of the three advanced oxidation technologies. The UV-LEDs advanced oxidation method provided a better reduction in SUVA values, with UV-LEDs/Cl_2 reducing SUVA to a greater extent than UV-LEDs/H_2O_2. The improved result of chlorine reaction compared to hydrogen peroxide reaction may be since the wavelength of the UV-LEDs used is 280 nm, which is a wavelength that for chlorine is more likely to stimulate the free radicals to complete the advanced oxidation due to its absorbance. In the case of THMFP, ozone outperformed UV-LEDs, but the dose range of UV and oxidants and the impact on THMFP, and the ratio of UV to oxidant in this work were limited. Additional experiments are needed to understand whether there is an optimum UV to oxidant ratio that minimizes THMFP. And technical limitations prevented UV-LEDs-related reactions from being accomplished in the same way as ozone reactions, and UV experiments under flow-through conditions were needed to solidify the conclusions of this experiment regarding DBPFP.

The comparison of UV-LEDs equipment with ozone technology in the field of water treatment is not entirely limited to treatment effectiveness – a more resilient treatment system to cope with future drinking water challenges notably source waters with high organic matter content that are more difficult to treat. Therefore, cost, ease of installation and environmental impact should all be considered when considering AOPs technology. Although UV-LEDs technology is not yet mature compared to ozone technology, it has

greater potential and is particularly advantageous in terms of energy consumption, cost and environmental friendliness (Farzanehsa et al., 2023; Toor & Mohseni, 2007).

5.2 Recommendation

Based on the results of this study, some recommendations will be provided for further research in this section.

The GAC-related experiments during this work were completed during the time period when the GAC was exhausted in the pilot plant, and subsequent experiments could be considered to be completed using new GAC media (Anderson et al., 2023). Experiments with UV-LED AOPs in combination with GAC at the same time showed good potential in some studies, far exceeding the effects of AOPs-only or GAC-only treatments (Toor & Mohseni, 2007). However, whether UV-LEDs AOPs can delay the exhaustion of GAC is worth exploring and deserves more research in the future.

More combinations of UVLED fluence to oxidant ratios should be tested to validate many of the conclusions in this paper and other experiments, particularly regarding the impact on DBPFP. The results of some studies indicated that higher intensity UV-related AOPs could reduce THMFP, and conducting similar experiments with UV-LEDs may be able to refine the experimental results of this study (Matilainen & Sillanpää, 2010; Parsons, 2004). Testing of DBPs was completed under only one condition per advanced oxidation due to experimental time constraints. More conditions can be considered to give more references for practical applications.

In order to better explore the principles and optimal operating conditions of different AOPs, measurements on free radicals associated with ozone and UV-LED/Cl_2 reactions should

be performed in the future. The determination of the chlorine reaction with the simultaneous action of multiple free radicals is of particular importance (Tian et al., 2020; Yin, Zhong, et al., 2018). Due to the improved control of the wavelength through UV-LEDs and the fact that the wavelengths were found to produce different advanced oxidizing effects for different oxides in this study, it is possible to further explore which are the most suitable wavelengths for the reaction of AOPs for different oxides, respectively.

The limitations of bench-scale research are still significant, and UV-LED AOPs will be more valuable as the technology advances to complete pilot-scale research and full-scale research to put UV-LEDs AOPs works into practical use.

Reference

Anderson, L. E., DeMont, I., Dunnington, D. D., Bjorndahl, P., Redden, D. J., Brophy, M. J., & Gagnon, G. A. (2023). A review of long-term change in surface water natural organic matter concentration in the northern hemisphere and the implications for drinking water treatment. Science of The Total Environment, 858, 159699. https://doi.org/10.1016/j.scitotenv.2022.159699

Anderson, L. E., Krkošek, W. H., Stoddart, A. K., Trueman, B. F., & Gagnon, G. A. (2017). Lake Recovery Through Reduced Sulfate Deposition: A New Paradigm for Drinking Water Treatment. *Environmental Science & Technology*, *51*(3), 1414–1422. https://doi.org/10.1021/acs.est.6b04889

Anderson, L. E., Tchonlla, M., Earle, M., Swinamer, R., & Gagnon, G. A. (2023). Adapting direct filtration to increasing source water dissolved organic carbon using clarification and granular activated carbon. *AWWA Water Science*, *5*(5), e1352. https://doi.org/10.1002/aws2.1352

Andreozzi, R., Caprio, V., Insola, A., & Marotta, R. (1999). Advanced oxidation processes (AOP) for water purification and recovery. *Catalysis Today*, *53*(1), 51–59. https://doi.org/10.1016/S0920-5861(99)00102-9

Beck, S. E., Ryu, H., Boczek, L. A., Cashdollar, J. L., Jeanis, K. M., Rosenblum, J. S., Lawal, O. R., & Linden, K. G. (2017). Evaluating UV-C LED disinfection performance and investigating potential dual-wavelength synergy. *Water Research*, *109*, 207–216. https://doi.org/10.1016/j.watres.2016.11.024

Beltrán, F. J., Ovejero, G., & Acedo, B. (1993). Oxidation of atrazine in water by ultraviolet radiation combined with hydrogen peroxide. *Water Research*, *27*(6), 1013–1021. https://doi.org/10.1016/0043-1354(93)90065-P

Bolton, J. R., & Linden, K. G. (2003). Standardization of Methods for Fluence (UV Dose) Determination in Bench-Scale UV Experiments. *Journal of Environmental Engineering*, *129*(3), 209–215. https://doi.org/10.1061/(ASCE)0733-9372(2003)129:3(209)

Boorman, G. A. (1999). Drinking water disinfection byproducts: Review and approach to toxicity evaluation. *Environmental Health Perspectives*, *107*(suppl 1), 207–217. https://doi.org/10.1289/ehp.99107s1207

Bridgeman, J., Bieroza, M., & Baker, A. (2011). The application of fluorescence spectroscopy to organic matter characterisation in drinking water treatment. *Reviews in Environmental Science and Bio/Technology*, *10*(3), 277–290. https://doi.org/10.1007/s11157-011-9243-x

Bridgewater, L. L., Baird, R. B., Eaton, A. D., Rice, E. W., American Public Health Association, American Water Works Association, & Water Environment Federation (Eds.). (2017). *Standard methods for the examination of water and wastewater* (23rd edition). American Public Health Association.

Budd, G. C., Hess, A. F., Shorney-Darby, H., Neemann, J. J., Spencer, C. M., Bellamy, J. D., & Hargette, P. H. (2004). Coagulation applications for new treatment goals. *Journal AWWA*, *96*(2), 102–113. https://doi.org/10.1002/j.1551-8833.2004.tb10559.x

Canada, H. (2014, October 22). *Guidelines for Canadian Drinking Water Quality—Summary Tables* [Guidance]. https://www.canada.ca/en/health-canada/services/environmental-workplace-health/reports-publications/water-quality/guidelines-canadian-drinking-water-quality-summary-table.html

Chen, W., Westerhoff, P., Leenheer, J. A., & Booksh, K. (2003). Fluorescence Excitation−Emission Matrix Regional Integration to Quantify Spectra for Dissolved Organic Matter. *Environmental Science & Technology*, *37*(24), 5701–5710. https://doi.org/10.1021/es034354c

Cheng, Z., Ling, L., Wu, Z., Fang, J., Westerhoff, P., & Shang, C. (2020). Novel Visible Light-Driven Photocatalytic Chlorine Activation Process for Carbamazepine Degradation in Drinking Water. *Environmental Science & Technology*, *54*(18), 11584–11593. https://doi.org/10.1021/acs.est.0c03170

Chow, C. W. K., van Leeuwen, J. A., Fabris, R., & Drikas, M. (2009). Optimised coagulation using aluminium sulfate for the removal of dissolved organic carbon. *Desalination*, *245*(1), 120–134. https://doi.org/10.1016/j.desal.2008.06.014

Clesceri, L. S., Eaton, A. D., Greenberg, A. E., Franson, M. A. H., American Public Health Association., American Water Works Association., & Water Environment Federation. (1996). *Standard methods for the examination of water and wastewater: 19th edition supplement* (19th ed). American Public Health Association.

Coble, P. G., Lead, J., Baker, A., Reynolds, D. M., & Spencer, R. G. M. (2014). *Aquatic Organic Matter Fluorescence*. Cambridge University Press. http://ebookcentral.proquest.com/lib/dal/detail.action?docID=1642336

Daniel, D., & Technologies, A. (n.d.). *Determination of Haloacetic Acids in Drinking Water by LC/MS/MS*.

Delpla, I., Jung, A.-V., Baures, E., Clement, M., & Thomas, O. (2009). Impacts of climate change on surface water quality in relation to drinking water production. *Environment International*, *35*(8), 1225–1233. https://doi.org/10.1016/j.envint.2009.07.001

DeMont, I., Stoddart, A. K., & Gagnon, G. A. (2021). Assessing strategies to improve the efficacy and efficiency of direct filtration plants facing changes in source water quality from anthropogenic and climatic pressures. *Journal of Water Process Engineering*, *39*, 101689. https://doi.org/10.1016/j.jwpe.2020.101689

Dobrović, S., Juretić, H., & Ružinski, N. (2007). Photodegradation of Natural Organic Matter in Water with UV Irradiation at 185 and 254 nm: Importance of Hydrodynamic Conditions on the Decomposition Rate. *Separation Science and Technology*, *42*(7), 1421–1432. https://doi.org/10.1080/01496390701289849

Dongsheng, W., Hong, L., Chunhua, L., & Hongxiao, T. (2006). Removal of humic acid by coagulation with nano-Al13. *Water Supply*, *6*(1), 59–67. https://doi.org/10.2166/ws.2006.007

Duan, J., & Gregory, J. (2003). Coagulation by hydrolysing metal salts. *Advances in Colloid and Interface Science*, *100–102*, 475–502. https://doi.org/10.1016/S0001-8686(02)00067-2

Edzwald, J. K. (1993). Coagulation in Drinking Water Treatment: Particles, Organics and Coagulants. *Water Science and Technology*, *27*(11), 21–35.

Eikebrokk, B., Vogt, R. D., & Liltved, H. (2004). NOM increase in Northern European source waters: Discussion of possible causes and impacts on coagulation/contact filtration processes. *Water Supply*, *4*(4), 47–54. https://doi.org/10.2166/ws.2004.0060

El Gamal, M., Mousa, H. A., El-Naas, M. H., Zacharia, R., & Judd, S. (2018). Bio-regeneration of activated carbon: A comprehensive review. *Separation and Purification Technology*, *197*, 345–359. https://doi.org/10.1016/j.seppur.2018.01.015

Elovitz, M. S., & Von Gunten, U. (1999). Hydroxyl radical/ozone ratios during ozonation processes. I. The R(ct) concept. *Ozone: Science and Engineering*, *21*(3), 239–260. Scopus. https://doi.org/10.1080/01919519908547239

Farzanehsa, M., Vaughan, L. C., Zamyadi, A., & Khan, S. J. (2023). Comparison of UV-Cl and UV-H2O2 advanced oxidation processes in the degradation of contaminants from water and wastewater: A review. *Water and Environment Journal*, *n/a*(n/a). https://doi.org/10.1111/wej.12868

Flaten, T. P. (2001). Aluminium as a risk factor in Alzheimer's disease, with emphasis on drinking water. *Brain Research Bulletin*, *55*(2), 187–196. https://doi.org/10.1016/S0361-9230(01)00459-2

Förster, H. (2004). UV/VIS Spectroscopy. In H. G. Karge & J. Weitkamp (Eds.), *Characterization I: -/-* (pp. 337–426). Springer. https://doi.org/10.1007/b94239

Ghosh, U., Weber, A. S., Jensen, J. N., & Smith, J. R. (1999). Granular Activated Carbon and Biological Activated Carbon Treatment of Dissolved and Sorbed Polychlorinated Biphenyls. *Water Environment Research*, *71*(2), 232–240. https://doi.org/10.2175/106143098X121761

Gil, A., Galeano, L. A., & Vicente, M. Á. (Eds.). (2019). *Applications of Advanced Oxidation Processes (AOPs) in Drinking Water Treatment* (Vol. 67). Springer International Publishing. https://doi.org/10.1007/978-3-319-76882-3

Gong, D.-Y., & Wang, S.-W. (2000). Severe summer rainfall in China associated with enhanced global warming. *Climate Research*, *16*(1), 51–59. https://doi.org/10.3354/cr016051

Goslan, E. H., Gurses, F., Banks, J., & Parsons, S. A. (2006). An investigation into reservoir NOM reduction by UV photolysis and advanced oxidation processes. *Chemosphere*, *65*(7), 1113–1119. https://doi.org/10.1016/j.chemosphere.2006.04.041

Heikkilä, A., Kärhä, P., Tanskanen, A., Kaunismaa, M., Koskela, T., Kaurola, J., Ture, T., & Syrjälä, S. (2009). Characterizing a UV chamber with mercury lamps for assessment of comparability to natural UV conditions. *Polymer Testing*, *28*(1), 57–65. https://doi.org/10.1016/j.polymertesting.2008.10.005

Hölz, K., Lietard, J., & Somoza, M. M. (2017). High-Power 365 nm UV LED Mercury Arc Lamp Replacement for Photochemistry and Chemical Photolithography. *ACS Sustainable Chemistry & Engineering*, *5*(1), 828–834. https://doi.org/10.1021/acssuschemeng.6b02175

Houghton, J. (2005). Global warming. *Reports on Progress in Physics*, *68*(6), 1343. https://doi.org/10.1088/0034-4885/68/6/R02

Hudson, N., Baker, A., & Reynolds, D. (2007). Fluorescence analysis of dissolved organic matter in natural, waste and polluted waters—A review. *River Research and Applications*, *23*(6), 631–649. https://doi.org/10.1002/rra.1005

Hur, J., Williams, M. A., & Schlautman, M. A. (2006). Evaluating spectroscopic and chromatographic techniques to resolve dissolved organic matter via end member mixing analysis. *Chemosphere*, *63*(3), 387–402. https://doi.org/10.1016/j.chemosphere.2005.08.069

Jarvis, P., Autin, O., Goslan, E. H., & Hassard, F. (2019). Application of Ultraviolet Light-Emitting Diodes (UV-LED) to Full-Scale Drinking-Water Disinfection. *Water*, *11*(9), Article 9. https://doi.org/10.3390/w11091894

Jarvis, P., Banks, J., Molinder, R., Stephenson, T., Parsons, S. A., & Jefferson, B. (2008). Processes for enhanced NOM removal: Beyond Fe and Al coagulation. *Water Supply*, *8*(6), 709–716. https://doi.org/10.2166/ws.2008.155

Jung, Y. J., Kim, W. G., Yoon, Y., Kang, J.-W., Hong, Y. M., & Kim, H. W. (2012). Removal of amoxicillin by UV and UV/H2O2 processes. *Science of The Total Environment*, *420*, 160–167. https://doi.org/10.1016/j.scitotenv.2011.12.011

Kerr, R. A. (2007). Global Warming Is Changing the World. *Science*, *316*(5822), 188–190. https://doi.org/10.1126/science.316.5822.188

Korotta-Gamage, S. M., & Sathasivan, A. (2017). A review: Potential and challenges of biologically activated carbon to remove natural organic matter in drinking water purification process. *Chemosphere*, *167*, 120–138. https://doi.org/10.1016/j.chemosphere.2016.09.097

Korshin, G. V., Benjamin, M. M., & Li, C.-W. (1999). Use of differential spectroscopy to evaluate the structure and reactivity of humics. *Water Science and Technology*, *40*(9), 9–16. https://doi.org/10.1016/S0273-1223(99)00634-4

Lamsal, R., Walsh, M. E., & Gagnon, G. A. (2011). Comparison of advanced oxidation processes for the removal of natural organic matter. *Water Research*, *45*(10), 3263–3269. https://doi.org/10.1016/j.watres.2011.03.038

Lanzarini-Lopes, M., Garcia-Segura, S., Hristovski, K., & Westerhoff, P. (2017). Electrical energy per order and current efficiency for electrochemical oxidation of p-chlorobenzoic acid with boron-doped diamond anode. *Chemosphere*, *188*, 304–311. https://doi.org/10.1016/j.chemosphere.2017.08.145

Leenheer, J. A., & Noyes, T. I. (1984). *A Filtration and Column-adsorption System for Onsite Concentration and Fractionation of Organic Substances from Large Volumes of Water*. U.S. Department of the Interior, U.S. Geological Survey.

Leenheer, J. A., Noyes, T. I., & Stuber, H. A. (1982). Determination of polar organic solutes in oil-shale retort water. *Environmental Science & Technology*, *16*(10), 714–723. https://doi.org/10.1021/es00104a015

Levchuk, I., Rueda Márquez, J. J., & Sillanpää, M. (2018). Removal of natural organic matter (NOM) from water by ion exchange – A review. *Chemosphere*, *192*, 90–104. https://doi.org/10.1016/j.chemosphere.2017.10.101

Liu, H., Zhang, B., Li, Y., Fang, Q., Hou, Z., Tian, S., & Gu, J. (2020). Effect of Radical Species and Operating Parameters on the Degradation of Sulfapyridine Using a UV/Chlorine System. *Industrial & Engineering Chemistry Research*, *59*(4), 1505–1516. https://doi.org/10.1021/acs.iecr.9b06228

MacIsaac, S. (2021). *ULTRAVIOLET LIGHT APPLICATIONS FOR THE DEGRADATION OF NATURAL ORGANIC MATTER IN WATER MATRICES* [Thesis]. https://DalSpace.library.dal.ca//handle/10222/80361

MacIsaac, S. A., Rauch, K. D., Prest, T., Simons, R. M., Gagnon, G. A., & Stoddart, A. K. (2023). Improved disinfection performance for 280 nm LEDs over 254 nm low-pressure UV lamps in community wastewater. *Scientific Reports*, *13*(1), Article 1. https://doi.org/10.1038/s41598-023-34633-7

Marda, S., Kim, D.-I., Kim, M.-J., Gordy, J., Pierpont, S., Gianatasio, J., Amirtharajah, A., & Kim, J.-H. (2008). Plant conversion experience: Ozone BAC process installation and disinfectant residual control. *Journal AWWA*, *100*(4), 117–128. https://doi.org/10.1002/j.1551-8833.2008.tb09608.x

Mathon, B., Coquery, M., Miege, C., Penru, Y., & Choubert, J.-M. (2017). Removal efficiencies and kinetic rate constants of xenobiotics by ozonation in tertiary treatment. *Water Science and Technology*, *75*(12), 2737–2746. https://doi.org/10.2166/wst.2017.114

Matilainen, A., Gjessing, E. T., Lahtinen, T., Hed, L., Bhatnagar, A., & Sillanpää, M. (2011). An overview of the methods used in the characterisation of natural organic matter (NOM) in relation to drinking water treatment. *Chemosphere*, *83*(11), 1431–1442. https://doi.org/10.1016/j.chemosphere.2011.01.018

Matilainen, A., & Sillanpää, M. (2010). Removal of natural organic matter from drinking water by advanced oxidation processes. *Chemosphere*, *80*(4), 351–365. https://doi.org/10.1016/j.chemosphere.2010.04.067

Matilainen, A., Vepsäläinen, M., & Sillanpää, M. (2010). Natural organic matter removal by coagulation during drinking water treatment: A review. *Advances in Colloid and Interface Science*, *159*(2), 189–197. https://doi.org/10.1016/j.cis.2010.06.007

Matsukawa, S., Itoho, S., Habuthu, S., & Aizawa, T. (2006). An approach to residual aluminium control at Nisiya purification plant, Water Works Bureau, Yokohama. *Water Supply*, *6*(4), 67–74. https://doi.org/10.2166/ws.2006.911

McDonough, L. K., O'Carroll, D. M., Meredith, K., Andersen, M. S., Brügger, C., Huang, H., Rutlidge, H., Behnke, M. I., Spencer, R. G. M., McKenna, A., Marjo, C. E., Oudone, P., & Baker, A. (2020). Changes in groundwater dissolved organic matter character in a coastal sand aquifer due to rainfall recharge. *Water Research*, *169*, 115201. https://doi.org/10.1016/j.watres.2019.115201

Meulemans, C. C. E. (1987). The Basic Principles of UV–Disinfection of Water. *Ozone: Science & Engineering*, *9*(4), 299–313. https://doi.org/10.1080/01919518708552146

Miralles-Cuevas, S., Darowna, D., Wanag, A., Mozia, S., Malato, S., & Oller, I. (2017). Comparison of UV/H2O2, UV/S2O82−, solar/Fe(II)/H2O2 and solar/Fe(II)/S2O82− at pilot plant scale for the elimination of micro-contaminants in natural water: An economic assessment. *Chemical Engineering Journal*, *310*, 514–524. https://doi.org/10.1016/j.cej.2016.06.121

Moreno-Castilla, C. (2004). Adsorption of organic molecules from aqueous solutions on carbon materials. *Carbon*, *42*(1), 83–94. https://doi.org/10.1016/j.carbon.2003.09.022

Muramoto, Y., Kimura, M., & Nouda, S. (2014). Development and future of ultraviolet light-emitting diodes: UV-LED will replace the UV lamp. *Semiconductor Science and Technology*, *29*(8), 084004. https://doi.org/10.1088/0268-1242/29/8/084004

Muruganandham, M., & Swaminathan, M. (2004). Photochemical oxidation of reactive azo dye with UV–H2O2 process. *Dyes and Pigments*, *62*(3), 269–275. https://doi.org/10.1016/j.dyepig.2003.12.006

Neal, C., Lofts, S., Evans, C. D., Reynolds, B., Tipping, E., & Neal, M. (2008). Increasing Iron Concentrations in UK Upland Waters. *Aquatic Geochemistry*, *14*(3), 263–288. https://doi.org/10.1007/s10498-008-9036-1

Newcombe, G., & Drikas, M. (1997). Adsorption of NOM onto activated carbon: Electrostatic and non-electrostatic effects. *Carbon*, *35*(9), 1239–1250. https://doi.org/10.1016/S0008-6223(97)00078-X

Park, J.-S., Choi, H., & Cho, J. (2004). Kinetic decomposition of ozone and para-chlorobenzoic acid (pCBA) during catalytic ozonation. *Water Research*, *38*(9), 2285–2292. https://doi.org/10.1016/j.watres.2004.01.040

Parsons, S. (2004). *Advanced Oxidation Processes for Water and Wastewater Treatment*. IWA Publishing.

Pi, Y., Schumacher, J., & Jekel, M. (2005). The Use of para-Chlorobenzoic Acid (pCBA) as an Ozone/Hydroxyl Radical Probe Compound. *Ozone: Science & Engineering*, *27*(6), 431–436. https://doi.org/10.1080/01919510500349309

Prasad, G., Kentilitisca, J. Y., Ramesh, M. V., & Suresh, N. (2020a). An Overview of Natural Organic Matter. In A. Kumar, M. Paprzycki, & V. K. Gunjan (Eds.), *ICDSMLA 2019* (pp. 1407–1416). Springer. https://doi.org/10.1007/978-981-15-1420-3_150

Prasad, G., Kentilitisca, J. Y., Ramesh, M. V., & Suresh, N. (2020b). An Overview of Natural Organic Matter. In A. Kumar, M. Paprzycki, & V. K. Gunjan (Eds.), *ICDSMLA 2019* (pp. 1407–1416). Springer. https://doi.org/10.1007/978-981-15-1420-3_150

Program, U. S. G. C. R. (2009). *Global Climate Change Impacts in the United States*. Cambridge University Press.

Quinlivan, P. A., Li, L., & Knappe, D. R. U. (2005). Effects of activated carbon characteristics on the simultaneous adsorption of aqueous organic micropollutants and natural organic matter. *Water Research*, *39*(8), 1663–1673. https://doi.org/10.1016/j.watres.2005.01.029

Rakness, K., Gordon, G., Langlais, B., Masschelein, W., Matsumoto, N., Richard, Y., Robson, C. M., & Somiya, I. (1996). Guideline for Measurement of Ozone Concentration in the Process Gas From an Ozone Generator. *Ozone: Science & Engineering*, *18*(3), 209–229. https://doi.org/10.1080/01919519608547327

Rekhate, C. V., & Srivastava, J. K. (2020). Recent advances in ozone-based advanced oxidation processes for treatment of wastewater- A review. *Chemical Engineering Journal Advances*, *3*, 100031. https://doi.org/10.1016/j.ceja.2020.100031

Rice, R. G. (1996). Applications of ozone for industrial wastewater treatment—A review. *Ozone: Science & Engineering*, *18*(6), 477–515. https://doi.org/10.1080/01919512.1997.10382859

Roback, S. L., Ishida, K. P., Chuang, Y.-H., Zhang, Z., Mitch, W. A., & Plumlee, M. H. (2021). Pilot UV-AOP Comparison of UV/Hydrogen Peroxide, UV/Free Chlorine, and UV/Monochloramine for the Removal of N-Nitrosodimethylamine (NDMA) and NDMA Precursors. *ACS ES&T Water*, *1*(2), 396–406. https://doi.org/10.1021/acsestwater.0c00155

Rook, J. (1972). Formation of haloform during chlorination of natural water. *Water Treatment and Examination*, *21*, 259.

Rosenfeldt, E. J., Linden, K. G., Canonica, S., & von Gunten, U. (2006). Comparison of the efficiency of OH radical formation during ozonation and the advanced oxidation processes O3/H2O2 and UV/H2O2. *Water Research*, *40*(20), 3695–3704. https://doi.org/10.1016/j.watres.2006.09.008

Rosenfeldt, E. J., Melcher, B., & Linden, K. G. (2005). UV and UV/H2O2 treatment of methylisoborneol (MIB) and geosmin in water. *Journal of Water Supply: Research and Technology-Aqua*, *54*(7), 423–434. https://doi.org/10.2166/aqua.2005.0040

Sarathy, S. R., & Mohseni, M. (2006). *An Overview of UV-based Advanced Oxidation Processes for Drinking Water Treatment*. *7*(1).

Satya Sai, P. M., Ahmed, J., & Krishnaiah, K. (1997). Production of Activated Carbon from Coconut Shell Char in a Fluidized Bed Reactor. *Industrial & Engineering Chemistry Research*, *36*(9), 3625–3630. https://doi.org/10.1021/ie970190v

Schaefer, R., Grapperhaus, M., Schaefer, I., & Linden, K. (2007). Pulsed UV lamp performance and comparison with UV mercury lamps. *Journal of Environmental Engineering and Science*, *6*(3), 303–310. https://doi.org/10.1139/s06-068

Selberg, A., Viik, M., Ehapalu, K., & Tenno, T. (2011). Content and composition of natural organic matter in water of Lake Pitkjärv and mire feeding Kuke River (Estonia). *Journal of Hydrology*, *400*(1), 274–280. https://doi.org/10.1016/j.jhydrol.2011.01.035

Sgroi, M., Anumol, T., Vagliasindi, F. G. A., Snyder, S. A., & Roccaro, P. (2021). Comparison of the new Cl2/O3/UV process with different ozone- and UV-based AOPs for wastewater treatment at pilot scale: Removal of pharmaceuticals and changes in fluorescing organic matter. *Science of The Total Environment*, *765*, 142720. https://doi.org/10.1016/j.scitotenv.2020.142720

Sharp, E. L., Parsons, S. A., & Jefferson, B. (2006). Seasonal variations in natural organic matter and its impact on coagulation in water treatment. *Science of The Total Environment*, *363*(1), 183–194. https://doi.org/10.1016/j.scitotenv.2005.05.032

Sheintuch, M., & Matatov-Meytal, Y. I. (1999). Comparison of catalytic processes with other regeneration methods of activated carbon. *Catalysis Today*, *53*(1), 73–80. https://doi.org/10.1016/S0920-5861(99)00104-2

Singer, P. C. (1994). Control of Disinfection By-Products in Drinking Water. *Journal of Environmental Engineering*, *120*(4), 727–744. https://doi.org/10.1061/(ASCE)0733-9372(1994)120:4(727)

Sommer, R., Haider, T., Cabaj, A., Pribil, W., & Lhotsky, M. (1998). Time dose reciprocity in UV disinfection of water. *Water Science and Technology*, *38*(12), 145–150. https://doi.org/10.1016/S0273-1223(98)00816-6

Song, K., Mohseni, M., & Taghipour, F. (2016). Application of ultraviolet light-emitting diodes (UV-LEDs) for water disinfection: A review. *Water Research*, *94*, 341–349. https://doi.org/10.1016/j.watres.2016.03.003

Srivastav, A. L., Patel, N., & Chaudhary, V. K. (2020). Disinfection by-products in drinking water: Occurrence, toxicity and abatement. *Environmental Pollution*, *267*, 115474. https://doi.org/10.1016/j.envpol.2020.115474

Steinberg, C. (2003). *Ecology of Humic Substances in Freshwaters: Determinants from Geochemistry to Ecological Niches*. Springer Science & Business Media.

Stoddart, A. K., & Gagnon, G. A. (2015). Full-Scale Prechlorine Removal: Impact on Filter Performance and Water Quality. *Journal AWWA*, *107*(12), E638–E647. https://doi.org/10.5942/jawwa.2015.107.0180

Sun, P., Lee, W.-N., Zhang, R., & Huang, C.-H. (2016). Degradation of DEET and Caffeine under UV/Chlorine and Simulated Sunlight/Chlorine Conditions. *Environmental Science & Technology*, *50*(24), 13265–13273. https://doi.org/10.1021/acs.est.6b02287

Sundstrom, D. W., Klei, H. E., Nalette, T. A., Reidy, D. J., & Weir, B. A. (1986). Destruction of Halogenated Aliphatics by Ultraviolet Catalyzed Oxidation with Hydrogen Peroxide. *Hazardous Waste and Hazardous Materials*, *3*(1), 101–110. https://doi.org/10.1089/hwm.1986.3.101

Suty, H., De Traversay, C., & Cost, M. (2004). Applications of advanced oxidation processes: Present and future. *Water Science and Technology*, *49*(4), 227–233. https://doi.org/10.2166/wst.2004.0270

Tang, H., Xiao, F., & Wang, D. (2015). Speciation, stability, and coagulation mechanisms of hydroxyl aluminum clusters formed by PACl and alum: A critical review. *Advances in Colloid and Interface Science*, *226*, 78–85. https://doi.org/10.1016/j.cis.2015.09.002

Taniyasu, Y., Kasu, M., & Makimoto, T. (2006). An aluminium nitride light-emitting diode with a wavelength of 210 nanometres. *Nature*, *441*(7091), Article 7091. https://doi.org/10.1038/nature04760

Thurman, E. M. (2012). *Organic geochemistry of natural waters*. Springer Science & Business Media.

Tian, F.-X., Ye, W.-K., Xu, B., Hu, X.-J., Ma, S.-X., Lai, F., Gao, Y.-Q., Xing, H.-B., Xia, W.-H., & Wang, B. (2020). Comparison of UV-induced AOPs (UV/Cl2, UV/NH2Cl, UV/ClO2 and UV/H2O2) in the degradation of iopamidol: Kinetics, energy requirements and DBPs-related toxicity in sequential disinfection processes. *Chemical Engineering Journal*, *398*, 125570. https://doi.org/10.1016/j.cej.2020.125570

Tichonovas, M., Krugly, E., Jankunaite, D., Racys, V., & Martuzevicius, D. (2017). Ozone-UV-catalysis based advanced oxidation process for wastewater treatment. *Environmental Science and Pollution Research*, *24*(21), 17584–17597. https://doi.org/10.1007/s11356-017-9381-y

Toor, R., & Mohseni, M. (2007). UV-H2O2 based AOP and its integration with biological activated carbon treatment for DBP reduction in drinking water. *Chemosphere*, *66*(11), 2087–2095. https://doi.org/10.1016/j.chemosphere.2006.09.043

Trueman, B. F., A. MacIsaac, S., K. Stoddart, A., & A. Gagnon, G. (2016). Prediction of disinfection by-product formation in drinking water via fluorescence spectroscopy. *Environmental Science: Water Research & Technology*, *2*(2), 383–389. https://doi.org/10.1039/C5EW00285K

Wang, W.-L., Wu, Q.-Y., Huang, N., Wang, T., & Hu, H.-Y. (2016). Synergistic effect between UV and chlorine (UV/chlorine) on the degradation of carbamazepine: Influence factors and radical species. *Water Research*, *98*, 190–198. https://doi.org/10.1016/j.watres.2016.04.015

WHITEHEAD, P. G., WILBY, R. L., BATTARBEE, R. W., KERNAN, M., & WADE, A. J. (2009). A review of the potential impacts of climate change on surface water quality. *Hydrological Sciences Journal*, *54*(1), 101–123. https://doi.org/10.1623/hysj.54.1.101

Woo, H. K., Nishijima, W., Baes, A. U., & Okada, M. (1997). Micropollutant removal with saturated biological activated carbon (BAC) in ozonation–BAC process. *Water Science and Technology*, *36*(12), 283–298. https://doi.org/10.2166/wst.1997.0458

Xiao, Y., Rohrlack, T., & Riise, G. (2020). Unraveling long-term changes in lake color based on optical properties of lake sediment. *Science of The Total Environment*, *699*, 134388. https://doi.org/10.1016/j.scitotenv.2019.134388

Xing, W., Ngo, H. H., Kim, S. H., Guo, W. S., & Hagare, P. (2008). Adsorption and bioadsorption of granular activated carbon (GAC) for dissolved organic carbon (DOC) removal in wastewater. *Bioresource Technology*, *99*(18), 8674–8678. https://doi.org/10.1016/j.biortech.2008.04.012

Xu, X.-R., Li, X.-Y., Li, X.-Z., & Li, H.-B. (2009). Degradation of melatonin by UV, UV/H2O2, Fe2+/H2O2 and UV/Fe2+/H2O2 processes. *Separation and Purification Technology*, *68*(2), 261–266. https://doi.org/10.1016/j.seppur.2009.05.013

Yamano, N., Kunisada, M., Kaidzu, S., Sugihara, K., Nishiaki-Sawada, A., Ohashi, H., Yoshioka, A., Igarashi, T., Ohira, A., Tanito, M., & Nishigori, C. (2020). Long-term Effects of 222-nm ultraviolet radiation C Sterilizing Lamps on Mice Susceptible to Ultraviolet Radiation. *Photochemistry and Photobiology*, *96*(4), 853–862. https://doi.org/10.1111/php.13269

Yang, W., Zhou, H., & Cicek, N. (2014). Treatment of Organic Micropollutants in Water and Wastewater by UV-Based Processes: A Literature Review. *Critical Reviews in Environmental Science and Technology*, *44*(13), 1443–1476. https://doi.org/10.1080/10643389.2013.790745

Yang, X., Lee, J., Yuan, L., Chae, S.-R., Peterson, V. K., Minett, A. I., Yin, Y., & Harris, A. T. (2013). Removal of natural organic matter in water using functionalised carbon nanotube buckypaper. *Carbon*, *59*, 160–166. https://doi.org/10.1016/j.carbon.2013.03.005

Yin, R., Blatchley, E. R. I., & Shang, C. (2020). UV Photolysis of Mono- and Dichloramine Using UV-LEDs as Radiation Sources: Photodecay Rates and Radical Concentrations. *Environmental Science & Technology*, *54*(13), 8420–8429. https://doi.org/10.1021/acs.est.0c01639

Yin, R., Ling, L., & Shang, C. (2018). Wavelength-dependent chlorine photolysis and subsequent radical production using UV-LEDs as light sources. *Water Research*, *142*, 452–458. https://doi.org/10.1016/j.watres.2018.06.018

Yin, R., Zhong, Z., Ling, L., & Shang, C. (2018). The fate of dichloroacetonitrile in UV/Cl 2 and UV/H 2 O 2 processes: Implications on potable water reuse. *Environmental Science: Water Research & Technology*, *4*(9), 1295–1302. https://doi.org/10.1039/C8EW00195B

Yoo, C., Jung, K.-S., & Kim, T.-W. (2005). Rainfall frequency analysis using a mixed Gamma distribution: Evaluation of the global warming effect on daily rainfall. *Hydrological Processes*, *19*(19), 3851–3861. https://doi.org/10.1002/hyp.5985

Yu, J., Wang, D., Yan, M., Ye, C., Yang, M., & Ge, X. (2007). Optimized Coagulation of High Alkalinity, Low Temperature and Particle Water: pH Adjustment and Polyelectrolytes as Coagulant Aids. *Environmental Monitoring and Assessment*, *131*(1), 377–386. https://doi.org/10.1007/s10661-006-9483-3

APPENDIX A: R Code for Plots

```
    # Q$#"  linear graph script


library(tidyverse)
library(reshape2)
library(ggthemes)
library(ggsci)
library(RColorBrewer)
library(dplyr)
setwd("F:/pCBA")
pCBA <- readxl::read_excel("pCBA JAY.xlsx", col_names = TRUE, skip = 0)
# plot:
pCBA$concentration <- as.numeric(pCBA$Concentration)
pCBA$pCBA1 <- as.numeric(pCBA$pCBA)
pCBA$pH <- as.factor(pCBA$pH)
pCBA$H2O2 <- as.factor(pCBA$H2O2)
# make ln column for finding k-values
data <- pCBA %>%
ggplot(aes(UV, concentration, fill = pH)) +
   facet_grid(H2O2 ~ pH) +
   geom_point(size=2, shape=23) +
   geom_smooth(method = "lm", se = FALSE, col = "black", linewidth = 0.5) +
   theme_bw()+
   ylab("Measured pCBA Concentration (μM)")+
   xlab("UV Fluence "~(mJ~cm^2))+
   scale_x_continuous(breaks=c(1000,500,100, 0))+
   theme(legend.position="none")
# extract linear model coefficients:
ggsave("pCBA.png", width=12, height=8, unit="in", dpi=1000)

pCBA$concentration <- as.numeric(pCBA$Concentration)
pCBA$pCBA <- as.numeric(pCBA$pCBA)
pCBA$pH <- as.factor(pCBA$pH)
pCBA$H2O2 <- as.factor(pCBA$H2O2)
# make ln column for finding k-values
data <- pCBA %>%
   ggplot(aes(UV, pCBA, fill = pH)) +
   facet_grid(H2O2 ~ pH) +
   geom_point(size=2, shape=23) +
   geom_smooth(method = "lm", se = FALSE, col = "black", linewidth = 0.5) +
   theme_bw()+
   ylab("ln(pCBA)")+
```

```
   xlab("UV Fluence "~(mJ~cm^2))+
   scale_x_continuous(breaks=c(1000,500,100, 0))+
   theme(legend.position="none")
# extract linear model coefficients:
       ggsave("lnpCBA.png", width=12, height=8, unit="in", dpi=1000)
```

```
       # AOPs SUVA script
        library(ggplot2)
       library(dplyr)
       library(lubridate)
       library(tidyverse)
       library(ggpubr)
       library(tidyr)
       library(mgcv)
       library(ggsci)
       library(patchwork)
       setwd("H:/AOP/SUVA")
```

```
AOPs <- read.csv("AOPs_J.csv")
AOPs$SUVA <- as.numeric(AOPs$SUVA)
AOPs$Location_Label <- as.factor(AOPs$Location_Label)
AOPs$UV_Dose <- as.factor(AOPs$UV_Dose)
AOPs$Oxidant_Dose <- as.factor(AOPs$Oxidant_Dose)
AOPs$Oxidant_Type <- as.factor(AOPs$Oxidant_Type)
AOPs$Treatment_Type <- as.factor(AOPs$Treatment_Type)


#x axis is UV dose
UV <- AOPs %>% filter(Location_Label %in% c("Sedimentation", "Ant/Sand", "GAC/Sand"), Oxidant_Type %in% c("H2O2", "Cl2")) %>%  mutate(Oxidant_Type = factor(Oxidant_Type, levels = c("H2O2", "Cl2"))) %>% mutate(Location_Label = factor(Location_Label, levels = c("Sedimentation", "Ant/Sand", "GAC/Sand"))) %>%
  ggplot(aes(x=as.factor(UV_Dose), y=SUVA, fill=Oxidant_Dose)) +
  geom_boxplot()+
  #geom_bar(stat="identity", position="dodge") +
  labs(fill="Oxidant Dose (mg/L)", color="Oxidant Dose (mg/L)")+
  theme_classic()+
  theme(axis.text.x = element_text(angle=45,hjust=1, face="bold"), axis.text.y = element_text(face="bold"), axis.title = element_text(face="bold", size=20), legend.position = "top", text = element_text(size = 20)) +
  scale_y_continuous(limits=c(0,3),
                     breaks=seq(0,3, 0.5))+
  facet_wrap(Oxidant_Type~Location_Label, ncol=3)+
  #geom_hline(aes(yintercept = SUVA_Untreated), linetype="dashed", color = "black") +
  xlab("UV Dose (mJ/cm2)")+
  ylab("SUVA (L-mg/m)")
ggsave("UVAOPs.png", width=12, height=8, unit="in", dpi=1000)


#x axis sample location
```

```
UV2 <- AOPs %>% filter(Location_Label %in% c("Sedimentation", "Ant/Sand", "GAC/Sand"), Oxidant_Type %in% c("H2O2", "Cl2"), Oxidant_Dose !="0") %>% mutate(Oxidant_Type = factor(Oxidant_Type, levels = c("H2O2", "Cl2"))) %>% mutate(Location_Label = factor(Location_Label, levels = c("Sedimentation", "Ant/Sand", "GAC/Sand"))) %>%
    ggplot(aes(x=as.factor(Location_Label), y=SUVA, fill=Oxidant_Dose)) +
    geom_boxplot()+
    #geom_bar(stat="identity", position="dodge") +
    labs(fill="Oxidant Dose (mg/L)", color="Oxidant Dose (mg/L)")+
    theme_classic()+
    theme(axis.text.x = element_text(angle=45,hjust=1, face="bold"), axis.text.y = element_text(face="bold"), axis.title = element_text(face="bold", size=20), legend.position = "top", text = element_text(size = 20)) +
    scale_y_continuous(limits=c(0,3),
                       breaks=seq(0,3, 0.5))+
    facet_wrap(Oxidant_Type~UV_Dose, ncol=4)+
    #geom_hline(aes(yintercept = SUVA_Untreated), linetype="dashed", color = "black") +
    xlab("Sample Location")+
    ylab("SUVA (L-mg/m)")
  ggsave("UVAOPs2.png", width=12, height=8, unit="in", dpi=1000)
```

```
Ozone <- AOPs %>% filter(Location_Label %in% c("Sedimentation", "Ant/Sand", "GAC/Sand"), Oxidant_Type =="Ozone") %>% mutate(Location_Label = factor(Location_Label, levels = c("Sedimentation", "Ant/Sand", "GAC/Sand"))) %>%
    ggplot(aes(x=as.factor(Oxidant_Dose), y=SUVA, fill=Oxidant_Dose)) +
    geom_boxplot()+
    #geom_bar(stat="identity", position="dodge") +
    labs(fill="Oxidant Dose (mg/L)", color="Oxidant Dose (mg/L)")+
    theme_classic()+
    theme(axis.text.x = element_text(angle=45,hjust=1, face="bold"), axis.text.y = element_text(face="bold"), axis.title = element_text(face="bold", size=20),
```

```
legend.position = "", text = element_text(size = 20)) +
        scale_y_continuous(limits=c(0,3),
                           breaks=seq(0,3, 0.5))+
        facet_wrap(~Location_Label, ncol=3)+
        xlab("Ozone Dose (mg/L)")+
        ylab("SUVA (L-mg/m)")
      ggsave("ozone.png", width=12, height=8, unit="in", dpi=1000)


      Ozone2 <- AOPs %>% filter(Location_Label %in% c("Sedimentation",
"Ant/Sand", "GAC/Sand"), Oxidant_Type =="Ozone") %>% mutate(Location_Label =
factor(Location_Label, levels = c("Sedimentation", "Ant/Sand", "GAC/Sand"))) %>%
        ggplot(aes(x=as.factor(Location_Label), y=SUVA, fill=Location_Label)) +
        geom_boxplot()+
        #geom_bar(stat="identity", position="dodge") +
        labs(fill="Oxidant Dose (mg/L)", color="Oxidant Dose (mg/L)")+
        theme_classic()+
        theme(axis.text.x = element_text(angle=45,hjust=1, face="bold"), axis.text.y =
element_text(face="bold"), axis.title = element_text(face="bold", size=20),
legend.position = "", text = element_text(size = 20)) +
        scale_y_continuous(limits=c(0,3),
                           breaks=seq(0,3, 0.5))+
        facet_wrap(~Oxidant_Dose, ncol=3)+
        xlab("Sample Location")+
        ylab("SUVA (L-mg/m)")
      ggsave("ozone2.png", width=12, height=8, unit="in", dpi=1000)
```

```
# AOPs DOC script


library(lubridate)
library(tidyverse)
library(ggpubr)
library(tidyr)
library(mgcv)
library(ggsci)
library(patchwork)
library(readxl)
library(ggplot2)
setwd("H:/AOP/SUVA")

AOP <- read.csv("UV254.csv")
AOP$DOC <- as.numeric(AOP$DOC)
AOP$Location_Label <- as.factor(AOP$Location_Label)
AOP$UV_Dose <- as.factor(AOP$UV_Dose)
AOP$Oxidant_Dose <- as.factor(AOP$Oxidant_Dose)
AOP$Oxidant_Type <- as.factor(AOP$Oxidant_Type)
AOP$Treatment_Type <- as.factor(AOP$Treatment_Type)

#x axis is UV dose
UV <- AOP %>% filter(Location_Label %in% c("Sedimentation",
"Ant/Sand", "GAC/Sand"), Oxidant_Type %in% c("H2O2", "Cl2")) %>%
mutate(Oxidant_Type = factor(Oxidant_Type, levels = c("H2O2",
"Cl2"))) %>% mutate(Location_Label = factor(Location_Label, levels =
c("Sedimentation", "Ant/Sand", "GAC/Sand"))) %>%
  ggplot(aes(x=as.factor(UV_Dose), y=DOC, fill=Oxidant_Dose)) +
  geom_boxplot()+
  #geom_bar(stat="identity", position="dodge") +
  labs(fill="Oxidant Dose (mg/L)", color="Oxidant Dose (mg/L)")+
  theme_classic()+
  theme(axis.text.x = element_text(angle=45,hjust=1, face="bold"),
axis.text.y = element_text(face="bold"), axis.title =
element_text(face="bold", size=20), legend.position = "top", text =
element_text(size = 20)) +
  scale_y_continuous(limits=c(1.2,2.5),
                     breaks=seq(1.2,2.5, 0.2))+
  facet_wrap(Oxidant_Type~Location_Label, ncol=3)+
  #geom_hline(aes(yintercept = SUVA_Untreated),
linetype="dashed", color = "black") +
  xlab("UV Dose (mJ/cm2)")+
```

```
        ylab("DOC(mg/L)")
      ggsave("UVaopDOC.png", width=12, height=8, unit="in", dpi=1000)

      Ozone <- AOP %>% filter(Location_Label %in% c("Sedimentation",
"Ant/Sand", "GAC/Sand"), Oxidant_Type =="Ozone") %>%
mutate(Location_Label = factor(Location_Label, levels =
c("Sedimentation", "Ant/Sand", "GAC/Sand"))) %>%
        ggplot(aes(x=as.factor(Oxidant_Dose), y=DOC,
fill=Oxidant_Dose)) +
        geom_boxplot()+
        #geom_bar(stat="identity", position="dodge") +
        labs(fill="Oxidant Dose (mg/L)", color="Oxidant Dose (mg/L)")+
        theme_classic()+
        theme(axis.text.x = element_text(angle=45,hjust=1, face="bold"),
axis.text.y = element_text(face="bold"), axis.title =
element_text(face="bold", size=20), legend.position = "", text =
element_text(size = 20)) +
        scale_y_continuous(limits=c(1.2,2.5),
                           breaks=seq(1.2,2.5, 0.2))+
        facet_wrap(~Location_Label, ncol=3)+
        xlab("Ozone Dose (mg/L)")+
        ylab("DOC(mg/L)")
      ggsave("ozonedoc.png", width=12, height=8, unit="in", dpi=1000)
```

```
      # THMFP script
      library(tidyverse)
      library(readxl)
      library(ggplot2)

      setwd("H:/AOP/DBPs/THM")
      dbp <- read_excel("THM JAY.xlsx", sheet='Sheet1')
      dbp$Value <- as.numeric(dbp$THM)
      dbp$Treament <- as.factor(dbp$Treatment_Type)

      dr %>% mutate(Treatment_Type=factor(Treatment_Type,
levels=c("Untreat water", "Ozone", "UV/H2O2", "UV/Cl"))) %>%
        ggplot(aes(x=Treatment_Type,
                   y=THM,)) +
        geom_boxplot()+
        theme(axis.text.x = element_text(angle=45,hjust=1, face="bold"),
              axis.text.y = element_text(face="bold"),
```

```
        axis.title = element_text(face="bold", size=20),
        text = element_text(size = 20)) +
  scale_y_continuous(limits=c(0,140), breaks=seq(0,140, 20))+
  xlab("Treatment")+
  ylab("THMFP(ug/L)")
ggsave("THM.png", width=12, height=8, unit="in", dpi=1000)
```

APPENDIX B: Table of Radicals Generation

Calculated *k*-values and R_{OH} for each reaction

H_2O_2(mg/L)	pH	k_d / k_{obs} (L mJ^{-1})	R_{OH} (10^{-14}M s L mJ^{-1})
0	5.5	2.36E-06	4.73E-02
	8	6.05E-06	1.21E-01
	10	5.86E-05	1.17E+00
1	5.5	8.90E-05	1.73E+00
	8	7.62E-05	1.40E+00
	10	6.37E-05	1.01E-01
10	5.5	2.42E-04	4.79E+00
	8	2.38E-04	4.64E+00
	10	1.98E-04	2.79E+00